

Ministério de Ciência, Tecnologia, Inovações e Comunicações  
Programa de Pós-Graduação em Astronomia



**Observatório  
Nacional**

## **Galaxy Evolution in Clusters and in the Field**

Julia de Figueiredo Gschwend

Monografia do Exame de Qualificação  
Aluna: Julia de Figueiredo Gschwend  
Orientador: Dr. Marcio Antonio G. Maia  
Curso: Doutorado em Astronomia  
Sorteio do tema: 14/09/2016  
Entrega: 14/11/2016  
Apresentação: 07/12/2016

## Abstract

Galaxies are distributed in regions with different spatial number densities. The two extreme environments, known as galaxy clusters and field, exhibit galaxies populations with remarkable differences in their properties. This is an evidence that the environment plays an important role in the evolutionary history of galaxies. While in clusters several violent environmental effects act upon the cluster members, in the field, galaxies are most likely to evolve passively experiencing secular processes. Several works have addressed the dependence of galaxy evolution on the environment, finding interesting clues about what, when and how the evolutionary processes happen in these two extreme environments. Such studies are mainly based on statistical tools like the luminosity and mass functions, or on the evolution of the fraction of a given galaxy type, both as a function of environment. The quenching of star formation activity and the migration in the color-magnitude diagram occurs in different timescales for objects with different masses and for those in different environments. In general, galaxy transformations in clusters happen first and quicker than in the field, so galaxy clusters can be considered as “catalysts” of galaxy evolution. Future surveys are promising since they will make it possible to look deeper in redshifts and to detect fainter objects. It allows expanding the limits of the investigations on galaxy formation and evolution, even for epochs when clusters were not yet assembled, and the environment was not yet critical for galaxy transformations.



# Chapter 1

## Introduction

The time scale of the transformations undergone by a galaxy is the order of million to billion years, impossible to be followed up on the human scale. However, due to the finite speed of light, it is possible to receive photons emitted in different epochs and therefore organize the observational data in a timeline. If we assume that the physics is the same elsewhere, studying statistically galaxy populations at different redshifts ( $z$ ), one can make assumptions about how galaxies evolve over the cosmic time. Large samples are demanded to explore the observables with a good representativity of galaxy populations and to ensure a robust statistics. In addition, in order to better understand the physical processes that are behind of the observed properties, it is also necessary to have detailed studies of smaller samples or even individual galaxies.

The information extracted from each redshift range can be faced like a puzzle piece. To visualize the big picture of Universe's history, it is necessary to observe deep, in a large range of redshifts. The so-called "pencil beam" surveys, e.g., the VIMOS VLT Deep Survey (VVDS, Le Fèvre et al., 2005), zCOSMOS Survey (Lilly et al., 2007), and DEEP2 Galaxy Redshift Survey (Newman et al., 2013), were designed for that purpose. Nonetheless, since the Universe is homogeneous only in very large scales, to avoid biases introduced by cosmic variance, it is also necessary to cover a large area. A good combination between area and depth is the ideal observational scenario for galaxy evolution studies.

Fortunately, in the last couple decades, several large surveys have been carried out, as the Sloan Digital Sky Survey (SDSS, York et al., 2000) and the Canada-France-Hawaii Telescope Legacy Survey (CFHTLS<sup>1</sup>). Some are in operation nowadays, as the Javalambre Physics of the Accelerating Universe Astrophysical Survey (J-PAS Benítez et al., 2014), the Dark Energy Survey (DES, Flaugher et al., 2005; Annis et al., 2005) and SDSS-IV (Eisenstein et al., 2011). Others are planned for the near future, as Dark Energy Spectroscopic Instrument (DESI), EUCLID (Content et al., 2008), and the Large Synoptic Survey Telescope (LSST, Ivezić et al., 2009). Most of these surveys were designed to investigate galaxy evolution — as it was, for instance, the Cosmic Evolution Survey(COSMOS, Scoville et al., 2007) and the Galaxy Evolution Explorer(GALEX, Bianchi et al., 1999)— but, their combination of area and depth provides a rich data set, very useful for such studies.

The combination of data from different sources is also a possible strategy to bypass the limitation of individual surveys. For instance, Conselice et al. (2016) used results from 13 previous works covering different redshift ranges to show that the total number density of galaxies is decreasing over the cosmic time ( $t$ ), proportionally to  $t^{-1}$ , and the total number of galaxies above  $10^6 M_{\odot}$  in the observable Universe is the order of  $2 \times 10^{12}$  (two trillion) up to  $z \sim 8$  (ten times higher than what would be observable, in a full sky survey, with the best current technology available). Another interesting example is the famous *Madau plot* (Madau et al., 1998; Madau and Dickinson, 2014). This plot is a compilation of star formation rate (SFR) measurements

---

<sup>1</sup><http://www.cfht.hawaii.edu/Science/CFHTLS>

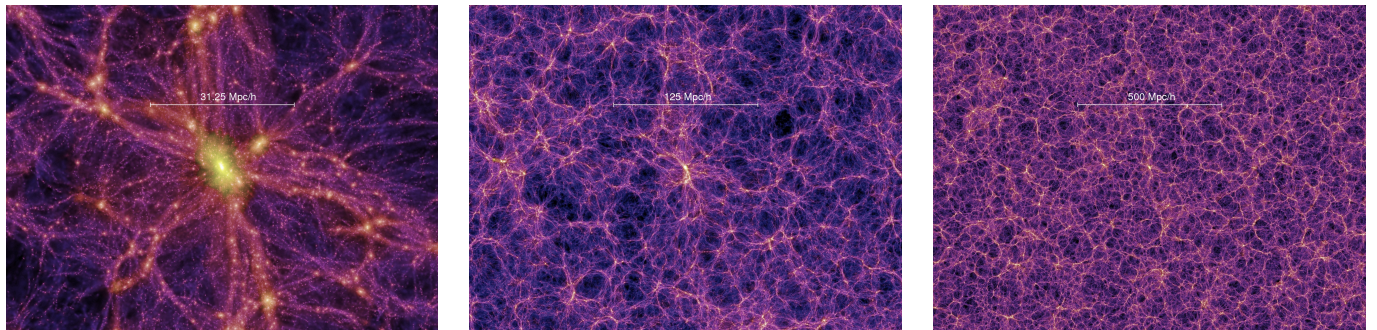


Figure 1.1: Snapshots of Millennium simulation, showing the typical degree of clustering for three different scales for the current age of the Universe. The scales from left to right are  $31.25$ ,  $125$ , and  $500 \text{ Mpc h}^{-1}$ .

in different wavelengths, from 14 works. It shows that the galaxy activity of convert gas into stars was increasing in the early Universe, reached a peak around  $z \sim 1.9$  (3.5 Gyr after the Big Bang), and is exponentially declining in later times. With this combination of data, Madau and Dickinson (2014) also inferred that before  $z \sim 1.3$ , half of the current total stellar mass was already assembled in stars and that there is an evidence in favor of the coevolution of black holes and their host galaxies.

Galaxies in our neighborhood exhibit a large variety of properties like size, color, shape, morphology, luminosity, surface brightness, star-formation activity, etc. Very deep images taken with the Hubble Space Telescope(HST), known as the Hubble Ultra Deep Field (HUDF, Beckwith et al., 2006), showed that the evolution was very strong in the first few billion years of the Universe. The star formation activity was already intense, even less than 1 billion year after the Big Bang. In the early Universe, galaxies were not so well defined morphologically as they are today. At that epoch, the young systems were mostly clumpy and irregular. As the Universe evolves, galaxies experience several transformations, resulting in a number of populations that share similar physical and structural properties. The main subject of galaxy evolution studies is precisely to understand the mechanisms responsible for led galaxies to this differentiation.

The origin of such mechanisms can be internal or external, as states the old *cliché* “nature versus nurture”. There are intrinsic processes occurring in galaxies that change its properties over time. That kind of physical phenomena would happen even if the galaxy was an isolated system e.g., the star formation, the aging of the stellar populations, active galactic nuclei (AGN) feedback, the formation of spiral arms and bars. On the other hand, there are also a lot of extrinsic processes, that strongly depends on the environmental influence e.g., ram-pressure stripping, galaxy harassment, strangulation and galactic cannibalism. There are several examples of observational features indicating that the environment plays an important role in the formation and evolution of galaxies. For instance, in high-density regions, we observe a red-sequence in the color-magnitude diagram (CMD), the presence of cD galaxies, the Butcher-Oelmer effect, etc (Mo et al., 2010). These and other aspects will be addressed in the next sections.

In the scale of tens or hundreds of  $\text{Mpc h}^{-1}$ , galaxies and dark matter halos are not homogeneously distributed. This is shown in Figure 1.1 with images from the Millennium Simulation<sup>2</sup> (Springel et al., 2005; Lemson and Virgo Consortium, 2006). They are distributed in filaments or sheets of overdense regions. Some amount of gas available in the intergalactic medium (IGM) also flows through this cosmic web. The almost empty regions between this structure are called “voids”. In the encounter of several filaments are the regions with the larger density of matter.

In extragalactic studies, the regions are often classified as one of the two extreme cases, based on the spatial density of galaxies: *clusters* and *field*. Nonetheless, many authors do not want to commit to a restricted definition of field and cluster, thus treating the two extreme environments

<sup>2</sup><http://wwwmpa.mpa-garching.mpg.de/galform/millennium/>

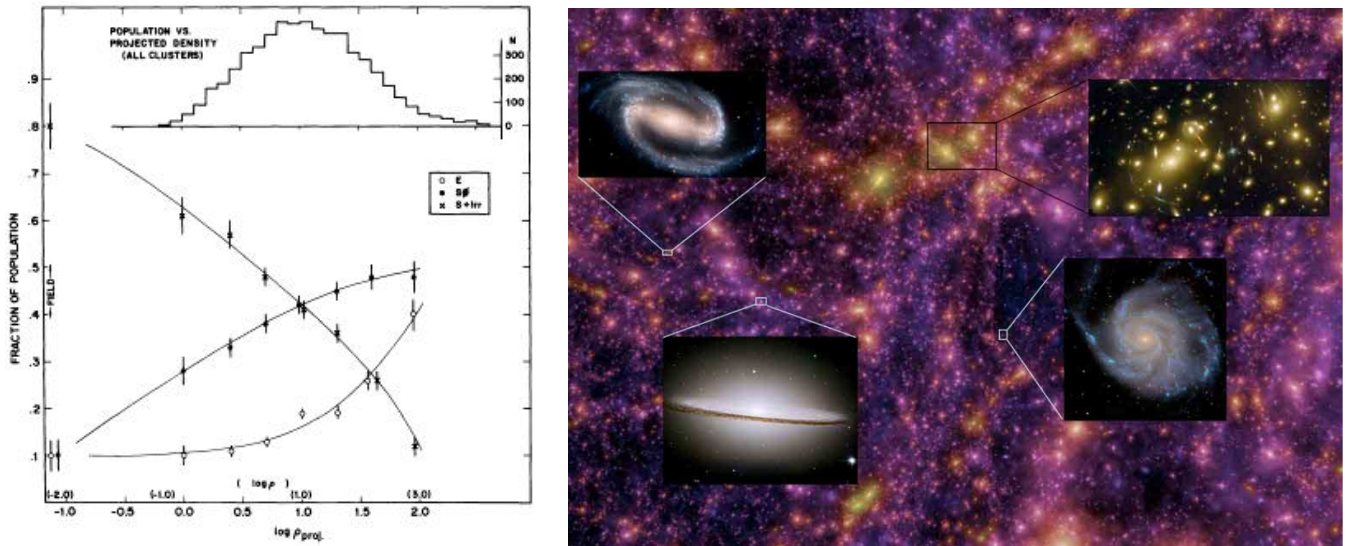


Figure 1.2: Left: the classic plot from (Dressler, 1980), addressing the fraction of galaxy population from the morphological types: elliptical (E), lenticular (S0), and spiral+irregular (S+Irr), as function of projected density. Right: Representation of the galaxy types that are preferably found in each environment, using a simulated image from the Millennium Simulation. (Figure from Kormendy (2013))

only as overdense and underdense regions. To investigate how the environment effects depend on time (or age of the Universe), it is necessary to observe cluster and field galaxies across the Universe, within a large redshift range, for sampling at different epochs. However, identifying cluster galaxies in the high- $z$  regime is by itself a big challenge, since, at the early epochs, these large systems were not assembled yet. Therefore, one has to identify not cluster, but the members of the progenitor system of a future cluster. For example, Venemans et al. (2007) have discovered six forming clusters of galaxies (protoclusters) from  $z \sim 5$  to  $\sim 2$ , by following-up Ly $\alpha$  emitter galaxies surrounding eight radio sources, using the same approach as done in previous works as in the series of papers started by Kurk et al. (2000).

In the local Universe, we do observe a clear dependence of galaxy properties on the environment. For instance, cluster galaxies are, in general, redder, gas poorer, more spheroidal (less “disky”), having less star-forming activity and smaller radii than the field counterparts. High-density regions are dominated by elliptical (redder) galaxies, while low-density environments are dominated by pure-disk (bluer) galaxies. Bulge-dominated disks, S0s, and barred galaxies are more often found in intermediate-density environments (Kormendy, 2013). This morphology-density relation was observed historically by Hubble and Humason (1931) and quantified after by Dressler (1980, see Figure 1.2). Recently, these results were confirmed by larger surveys and the dependence of galaxy evolution with the environment has been studied by observing several other features. Gerke et al. (2007) measured the fraction of blue galaxies in DEEP2 survey, for galaxies in groups and in the field, separately, confirming that the well-known color segregation observed in the local Universe is already in place at  $z \sim 1$ .

In the classic annual review of 1988, Binggeli et al. (1988) collected results from several works, showing that the luminosity functions (LFs) for the Hubble types ( $\Phi_T(M)$ ), separately, are very similar in the bright end, but substantially different in the faint end. For instance, spirals and S0s have nearly Gaussian LFs. Giant ellipticals have “skewed” Gaussian LFs, while dwarf spheroidals (at that time, classified as dwarf ellipticals) and irregular galaxies obey the Schechter parametrization of the LF. They also showed that the LF shape for a given type is almost independent of the environment, except for the relative proportions, which causes differences in the shape of the global LF (Figure 1.3). The type mixture in the given sample will define the bumps or depressions in the global LF shape. The faint-end is the most sensitive range to

differences in the proportions of that mixture, as all individual LFs are much more alike in the bright-end.

Recent works also have explored galaxy properties in clusters and in the field. For instance, Mei et al. (2009), studied the evolution of the color-magnitude relation, analyzing the red-sequence's scatter, slope, zero points, and fraction of morphological types, for a sample of eight galaxy clusters, from  $z \sim 0.8$  to  $z \sim 1.3$ . McNaught-Roberts et al. (2014) measured the dependence of the luminosity function (LF) on environment, redshift, and color. Balogh et al. (2001), Bolzonella et al. (2010), and more recently Mortlock et al. (2015) and Davidzon et al. (2016) studied the stellar mass function (MF) for galaxies in high-density and low-density environments, separately. The results of these works will be discussed in Chapter 4.

Instead of considering only two extreme environments, another possibility is to define a range of density bins ( $D$ ), so the LF is treated as a two-variable function,  $\Phi(M, D)$ . The latest results have shown that, rather than a hard separation between clusters and field, the LF varies smoothly as a function of the number overdensity (McNaught-Roberts et al., 2014).

When measurements of environment are not available, since this morphology-density relation (reflected in a color-density relation) is clearly observed, studies that treat red/blue or early/late-type galaxy populations separately (e.g., Faber et al., 2007; Loveday et al., 2012) can be used as a rough approximation for comparison between high and low-density environments, respectively.

Another interesting approach to understanding this red/blue dichotomy is the study of galaxies that are intermediate between these two populations: the inhabitants of the *green valley*. If galaxies migrate from blue to red population after ceasing their star formation activity, green galaxies would be objects caught during the transition. Mendez et al. (2011) confirmed that green valley objects are intermediate between blue and red galaxies, in terms of concentration, asymmetry, and morphological properties. The number deficit of observed green galaxies suggests that this migration occurs in a short time scale (Gonçalves et al., 2012). Assuming that there are galaxies falling into the gravitational well of galaxy clusters, the observation of green galaxies in overdense regions can bring hints about the environmental processes that contribute to quenching star formation.

The current works in galaxy evolution are trying to answer the following questions (and lots of other ones): What shuts off star formation in galaxies? How star-forming, spiral galaxies turn into quiescent, elliptical galaxies? What are the processes responsible for the build-up of the red

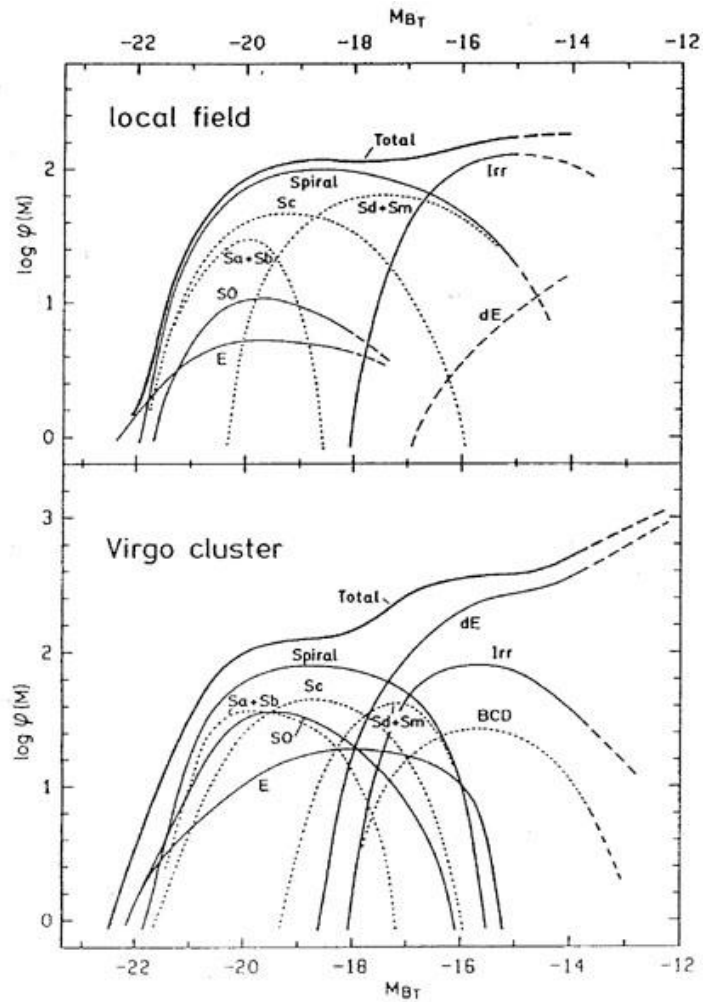


Figure 1.3: Classical figure from the Annual Review Binggeli et al. (1988). LF for the different Hubble types in arbitrary scale for two examples of low and high-density environments, the local field and the Virgo Cluster, respectively. Dashed lines are extrapolations for the fitted curves. Dotted lines are the LFs for two types combined. Caveat: spheroidal galaxies here were still called dwarf ellipticals (dEs).

sequence in clusters? When was the red sequence built up? What are the evolutionary paths followed by galaxies with different morphologies on the CMD? And finally, what is the role of the environment in all of this processes?

The present work is organized as follows: Chapter 2 addresses passive evolution processes and secular evolution of field galaxies; Chapter 3 presents some environmental effects on galaxies and galaxy evolution inside galaxy clusters. Chapter 4 shows a compilation of recent results collected from the literature, focused on observational works that compare galaxy evolution in different environments. Highlights from the previous chapters are found in Chapter 5. Since this is a bibliographic research, there is no original result presented. All the content presented here is based on scientific papers and textbooks.

## Chapter 2

# Galaxy Evolution in the Field

In the hierarchical or “bottom-up” scenario of Cold Dark Matter (CDM) theories, the dark matter halos grow-up by merging with each other. The more massive the dark matter halo becomes, the stronger is its gravitational potential, hence, its capacity to capture baryons to assemble galaxies (White and Rees, 1978).

Most galaxies formed in the field are disk galaxies, which are supported by rotation. It was very common for the primordial gas clouds to have some anisotropy in its velocity field during the collapse, and hence some amount of angular momentum. As the collapse evolves and more material is accreted, if the rotation component is relatively important, the system becomes flattened and forms a disk shape.

It is also possible to form elliptical galaxies, which are supported by velocity dispersion, in a monolithic collapse (Eggen et al., 1962). In this case, the gas falls into the dark matter halo very quickly, and the subsequent violent star formation burst consumes rapidly the gas reservoir. This process is much rarer and maybe would explain the formation of very massive elliptical galaxies, observed in the early Universe.

According to the CDM models, the halos keep on merging, whenever they encounter each other. If there are galaxies already formed within the halos, the baryonic matter merges too, forming a new central galaxy with the material from the two original ones. Sometimes one of the progenitors are much bigger than the other(s), and the accretion of the smaller halo doesn’t change much its structure (minor merger), including its dynamical properties. In this case, the smaller system(s) will orbit around the larger halo, experiencing tidal effects and dynamical friction, which remove material from its outer regions or even destroy it completely.

In other cases, the progenitors have approximately the same size and the merging process happens with a violent relaxation, rapidly transforming the kinetic energy into internal binding energy of the remnant (major merger). A major merger between two or more galaxies will generate an elliptical one. Depending on the amount of gas in the progenitors, the merger can be classified as “wet” (gas-rich), or “dry” (gas poor). The merger between two gas-poor elliptical progenitors will generate a new large elliptical. The merger between two gas-rich disks will also

---

<sup>1</sup>[http://people.virginia.edu/~dmw8f/astr5630/Topic02/Lecture\\_2.html](http://people.virginia.edu/~dmw8f/astr5630/Topic02/Lecture_2.html)

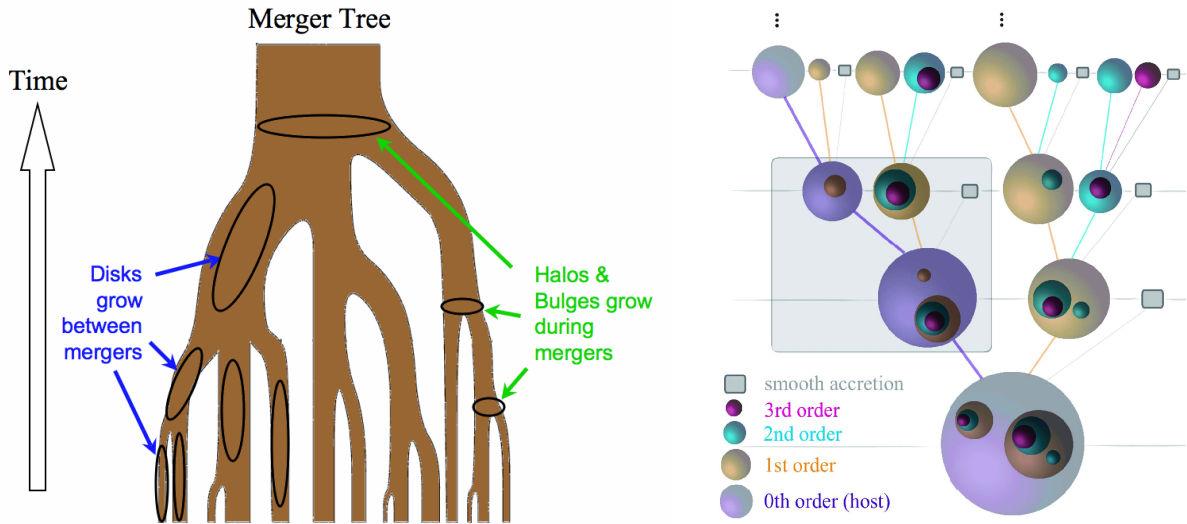


Figure 2.1: Left panel: a cartoon<sup>1</sup>that illustrates the concept of “Merger Tree”. Time increases from bottom-up. Right panel: figure from Jiang and van den Bosch (2014), a detailed illustration exemplifying the assembling history of a host halo (purple sphere at the bottom). Here time passes from top-down. The size of a sphere is proportional to its mass, while its color reflects its order, as indicated (the smaller order, the larger number of halos accreted).

generate an elliptical system. The merge “impact” compresses the gas, inducing a star formation burst, rapidly consuming the gas fuel. In cases like this, an AGN activity can be triggered with the build of the new galaxy. It is believed that most giant elliptical galaxies were formed via this mechanism.

The “Merger Tree”, a schematic concept for successive mergers building up large structures, is shown in Figure 2.1. The right panel, shown an illustration from Jiang and van den Bosch (2014) for a model of assembling dark matter halos. In the left panel, the thickness of branches represents the total mass (dark and baryonic matter). As halos merge, branches become thicker and structures grows. With time passing, if there is a disk galaxy in a branch, while it does not meet with other branches, it can accrete gas or little satellites, growing the disk. When the merger happens, the disk structure undergoes a disorganization, and an elliptical object is formed.

Eventually, the new system can accrete more cold gas and grow a new disk. In this case, the spheroidal component remnant from the merger will be considered a “classical bulge”. Elliptical galaxies and classical bulges have similar properties, being indistinguishable in several observational quantities. By comparing pairs of observables, they satisfy the same scale relations. For instance, the classical bulges and regular elliptical galaxies occupy the same *locus* in the relations between the absolute magnitude and Sérsic index or surface brightness, as shown in Figure 2.3. This is an evidence of their common formation history.

The hierarchical paradigm and the passive evolution coexist and their relative importance depends on the lookback time and the environment (Kormendy, 2013). As the Universe expands, the probability of encounters decreases. Most galaxies in low-density regions will continue to evolve passively and will never merge to another galaxy. These galaxies exchanges energy and matter with the IGM through inflow and outflow processes. Figure 2.2 shows a scheme of the evolution of an individual galaxy. The galaxy, represented by the dashed line, is a system composed of hot and cold gas, stars, and a super-massive black hole (SMBH). The arrows denote the energy transfer processes. Radiative cooling turns the hot gas into cold gas, so it can collapse to form stars. Star formation gives back energy, heating the surrounding gas, via UV emission, and supernova explosions, which also deliver mass and metals to the interstellar medium (ISM). The accretion of material by the SMBH can trigger an AGN, which also contributes to heat the gas and to eject mass and radiation, even for outside the galaxy, through jet outflows. So the

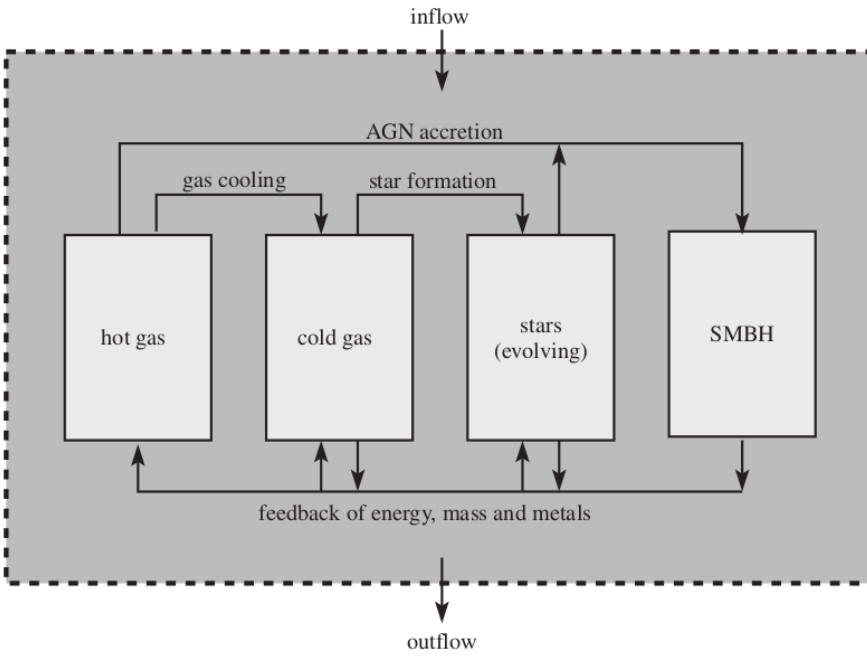


Figure 2.2: A representation of an individual galaxy (dashed rectangle) with its ingredients (light gray boxes) and main processes of energy exchange (arrows). Figure from the book Mo et al. (2010).

system is not necessarily a closed box, it is possible to happen inflow of gas from the IGM, and outflows due to SN and/or AGN activity. All these processes can be intensified or suppressed if the galaxy eventually merges or interacts with another galaxy (Mo et al., 2010).

## 2.1 Secular evolution in disk galaxies

Rather than the rapid change that happens in a protogalactic collapse or in a merge event, galaxies can go through several long-term transformations, known as *secular evolution*. The simple aging of stellar populations, making the galaxy systematically redder, duster and metal richer is, by itself, an example of the slow evolution of galaxy properties. The accretion of gas and little satellites works as a fuel to sustain the star formation activity for large periods of time. Even a “sleeping” AGN can be awakened in the case of the accretion of a gas-rich satellite.

The formation of spiral arms is also an example of a secular evolution process. There are a couple theories to explain this phenomenon. One of the most accepted claims that density waves propagate in large time-scales, compressing the cold gas available, thus boosting star-formation activity in specific regions of the disk (Kormendy, 2013). The spiral structure would be a quasi-stationary density wave that rotates at a constant angular velocity, different from the disk. Stars in the inner parts of the disk rotate faster than the pattern, passing the wave, while stars in the outer parts of the galaxy move slower, being passed by the wave (Lin and Shu, 1966).

The arm configures a gravitational potential well, so stars speed up toward the arm when getting closer, and slow down when leaving it. Hence, stars spend more time around the density wave that is amplified by self-gravity. Cold gas also is also compressed along the density wave, which boosts the star formation in these regions, making the pattern easily detectable. On the concave side of the arms, there are very dusty clouds of molecular gas, forming stars. Next, there are bright HII regions with young OB stars, that have passed through their birth-clouds and the older stars are on the convex side of the arm.

The causes for the start of the density perturbations are not completely understood. Some hypotheses connect formation of spiral arms to initial asymmetries in the disk formation, a presence of bars or oval disks, infall of gas clouds and environmental processes. Also, there are alternative theories to explain the formation of the spiral arms. In *chaotic theory*, the random star-forming activity above average would be propagated in the disk due to differential rotation.

In the *tidal driven theory*, where the arms would be a two-sided response to a perturbation, consequence of an interaction with another galaxy. In the self-propagation theory, supernova blast waves would be the responsible to compress the gas, triggering star formation bursts in a chain reaction. The arm structure would also be propagated by differential rotation. Nevertheless the density wave theory still the one that best explains the structure in spirals with well-defined arms, so-called grand design galaxies (Kormendy, 2013).

Another example of a secular process is the growth, evolution, and death of bars. Bars are a structural component observed in the central part of  $\sim 2/3$  of disk galaxies (Eskridge et al., 2000). Although they are located in the same region as the bulge, and they are predominantly formed by old stars, the bars are a phenomenon that belongs to the disk, which is confirmed by its strong rotation component. The bars develop spontaneously from gravitational instabilities in the rotating disk, concentrating material in an elongated structure that rotates linked to the spiral arms (when it exists). They tend to live for a finite period of time since it forces gas to fall toward the galactic center, forming a high-density environment (“pseudo-bulge”) that weakens itself. The death of the bar happens with the escape of stars, forming a lens structure of low surface brightness. The formation of pseudo-bulges in the galactic center is not always followed by the formation of a bar. These structures are the result of the accumulation of material in the galactic center, forming a high-density central component, which grows slowly out of the disks, not rapidly by galaxy mergers, as a classical bulge.

Pseudo and classical bulges present substantial differences in its physical properties. The firsts are flatter and more rotation-dominated, having a small velocity dispersion, for their luminosity. They show ongoing star formation, so their color is closer to the disk’s color than a classical bulge. Most pseudo-bulges have low bulge-to-total luminosity ratio ( $PB/T < 1/3$ ), in comparison to the typical values for classical bulges ( $B/T > 1.2$ ). Pseudo-bulges do not correlate with supermassive black holes, like classical bulges and ellipticals do. The light profile is also an indicator of the bulge’s nature. Pseudo-bulges typically have Sérsic index ( $n$ )  $< 2$ , while classical ones have  $n > 2$ , as shown in Figure 2.3.

It is possible that classical and pseudo-bulges coexist in the same galaxy. The presence of bars in bulge-dominated galaxies, suggests that matter concentration from disc dynamical instabilities can occur in systems that host classical merger-built bulges (Kormendy and Kennicutt, 2004). Alternatively, there is a none negligible amount of galaxies with no bulge at all. The explanation for the existence of pure disks remains a challenge for galaxy formation theories. It is easier to explain dwarf pure disks since they suffer fewer mergers, they tend to accrete gas in cold streams, and they are more sensitive to supernova feedback. On the other hand, giant pure disks should not exist, but they are actually observed. Galaxy mergers are expected to happen often enough so that every giant galaxy should have a classical bulge (Kormendy, 2013).

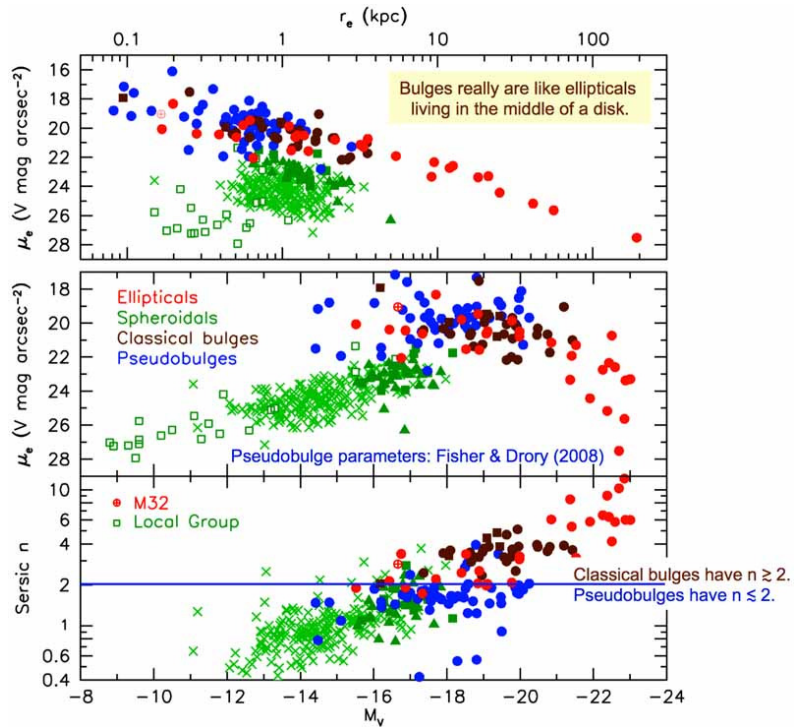


Figure 2.3: Plot from Kormendy (2013): structural parameter correlations for ellipticals (red), spheroidals galaxies (green), classical bulges (brown), and pseudo-bulges (blue). Top panel: effective surface brightness  $\mu_e$  versus effective radius  $r_e$ . Middle and bottom panels: Sérsic index  $n$  and  $\mu_e$ , respectively, versus galaxy or bulge absolute magnitude.

Very roughly speaking, the life history of a field galaxy is believed to follow the steps: merge of dark matter halos containing gas; collapse and accretion of gas clouds; flattening to a disk shape, due to angular momentum, if it is important. If not, the system evolves as an irregular galaxy; continued star-forming (several generations, producing metals and dust); feedback via supernovae and/or AGN activity; more gas accretion from cold streams and accretion of gas-rich dwarfs; more gas cooling, more star formation; possible secular processes, which can happen repeated times in large time-scales, as the growth of a pseudo-bulge, formation of a bar, rings, lens, spiral arms, etc; eventually, a possible major merger, drastically transforming the disk into an elliptical galaxy; eventually more gas accretion, transforming the elliptical system into a classical bulge; aging and reddening of stellar populations and... What comes later? What can be expected/predicted to be the fate of disks and irregular systems that are passively evolving?

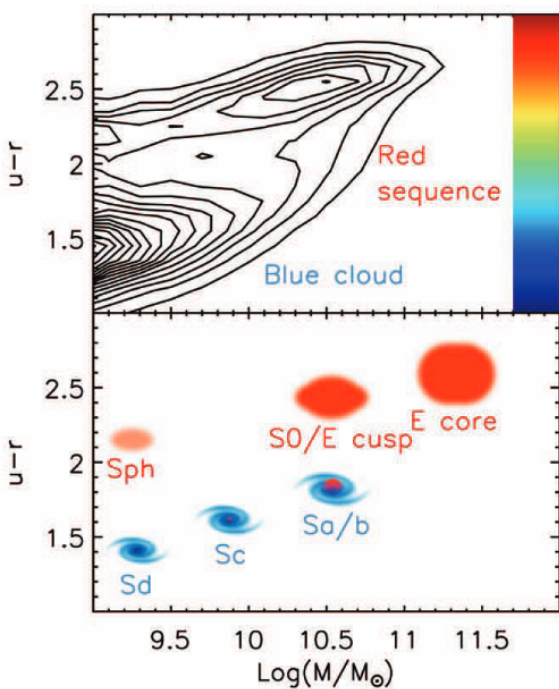


Figure 2.4: Color vs. mass. Top: density contours. Bottom: the correspondence with the dominant morphological types for each region of the diagram. Figure from Kormendy (2013).

S0 and Sph are continuous in the parameter relations, pointing that Sph are bulgeless S0s.

Figure 2.4 shows a color-mass diagram (CMD, or equivalently, magnitude rather than mass) and the correspondence with the dominant morphological types in each combination of the two parameters. In the upper panel, the density contours evidence the two main galaxy populations: the red sequence and the blue cloud. The bright end of the red sequence is mostly populated by giant ellipticals with a core, i.e., missing light compared to the extrapolation of Sérsic fit in the light profile. The center of the red sequence is predominantly composed by S0s and cuspy ellipticals, those with extra light compared to the extrapolation of Sérsic fit. A third dense region in the diagram lies on the faint end of the red sequence, approximately at  $(\log M/M_\odot, u-r)=(9.0, 2.2)$ , that is populated by the spheroidal galaxies. The migration from the blue cloud for that region is not supposed to happen via mergers, as it is at the bright end.

This new paradigm supports the revision of the Hubble Classification Scheme, as done by Kormendy and Bender (1996) (Figure 2.5). On the left, the elliptical galaxies, that were formed by mergers. On the right, two categories of disks. In the bottom sequence, the active star-forming ordinary and barred spirals, following the same criteria as used in Hubble Scheme of the relative

When E. Hubble propose the “tuning fork” morphological classification scheme, astronomers believed that spiral galaxies were an evolved version of ellipticals. That is the historical reason for the names “early” and “late”-types. Even though people realized that this is not true, this nomenclature has remained widely used by the community. Nowadays it is believed that spheroidal (Sph) galaxies are “red and dead” late-type spiral and irregular galaxies (Larson et al., 1980). Historically, the dwarf spheroidals (dSph) observed in our neighborhood were misclassified as dwarf ellipticals (dE), due to its isophotal profile looks like the elliptical morphology. However, besides the lower surface brightness, exploring the correlations between several observational properties, it became clear that the Sph lies on a different track compared to ellipticals and classical bulges (see again Figure 2.3, where spheroidal galaxies are represented by green points).

The relation between size and density indicates that the Sph have a formation history similar to disks and irregulars, distinct from ellipticals. dSph and dIrr should have a similar history, but dSph have no star formation activity, indicating that dSph are quenched dIrr. S0 galaxies are smoothed disks, with elliptical isophotes.

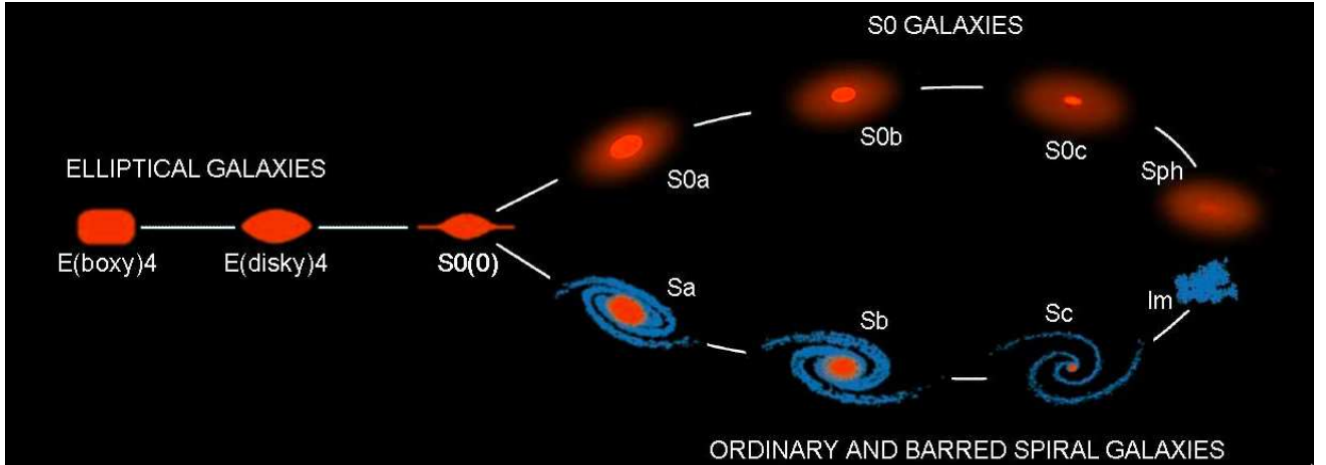


Figure 2.5: Revised Hubble's classification scheme, proposed by Kormendy and Bender (1996). Figure updated in Kormendy and Bender (2012).

importance of the bulge (Sa, Sb, Sc..), ending with the irregular galaxies, now interpreted as star-forming bulgeless systems. In addition, there is a parallel sequence of S0 galaxies, being interpreted as quenched disks with the same possibilities of B/T ratio as the spirals (forming the sequence S0a, S0b, S0c..), ending with the spheroidal galaxies, now interpreted as a bulgeless S0. The upper sequence is supposed to be the future of the lower sequence, if only passive evolution happen. Transitional objects between spirals and S0s exist but are not illustrated. This scheme comprehends the large majority of morphologies found in the local Universe, however still exists a small fraction of peculiar galaxies that does not fit in these groups. Most of them are an interacting pair of galaxies or even an ongoing merger.

## Chapter 3

# Galaxy Evolution in Clusters

Galaxy clusters are the largest gravitationally bound systems in the Universe. They began to form at earlier times, as a large-scale effect of the hierarchical assembling of matter, reaching masses the order of  $\mathcal{M} \lesssim 10^{14} \mathcal{M}_\odot$ . In very large scales, clusters are homogeneously distributed, the typical spatial density is 1 cluster per  $10^5$  to  $10^6$  Mpc $^3$ ,  $\sim 10^3$  to  $10^4$  times rarer than typical galaxies. The first clusters detections were based on the projected density, measured from optical images in photographic plates. One of the first important cluster catalogs, compiled by Abell (1958), included  $\sim 4$  k rich clusters of galaxies in both hemispheres. At that epoch, the observational limitations constrained the samples to have mostly neighbor systems in the local Universe.

Currently, there are a variety of techniques to find clusters that are effective, even for those very distant systems. For instance, search for overdensities in a 3D spatial map (e.g., Miller et al., 2005), search for red sequences using optical/IR surveys (e.g., Gladders and Yee, 2000; Rykoff et al., 2014), search for hot and luminous X-ray emitting halo (using space telescopes

like Chandra X-ray Observatory or XMM-Newton), search for Sunyaev-Zeldovich effect using cosmic microwave background experiments (South Pole Telescope, Planck), and in future, usage of gravitational lensing (e.g., EUCLID mission, planned to start in  $\sim$ 2020).

### 3.1 Galaxies are affected by the environment

As mentioned in Chapter 1, galaxy clusters are very rich in early-type galaxies, compared to lower-density regions. The average fraction of E + S0 galaxies is  $\sim 80\%$  in relaxed clusters, and  $\sim 50\%$  in young clusters, while it is  $\sim 30\%$  in the field (Mei et al., 2009; Mo et al., 2010). These early-type galaxies form a narrow red sequence in the cluster's CMD. This color-magnitude relation can be related to age and/or metallicity. Older galaxies, that are redder due to natural stellar evolution, would be also the more massive ones because they are assembling mass for longer. On the other hand, massive galaxies are more able to avoid the escape of metals during supernova explosions and stellar winds, due to their stronger gravity field (Ellis et al. 1997). Hence, the larger the width of the red sequence, the greater the range of ages and/or metallicities of cluster members (Mei et al., 2009). There is no strong variation on the slope of the red sequence in CMD in the range from  $z \sim 1$  to  $z = 0$ . The passive evolution of stellar populations in the elliptical galaxies causes a translation of the red sequence to a redder locus in CMD with time.

The radial distribution of galaxies in a cluster roughly follows that of the dark matter, but massive, red and early-type are much more centrally concentrated than the less massive, blue, late-type galaxies. The fraction of elliptical and S0 galaxies is larger in the inner parts of the clusters, where the density of galaxies is larger. This fraction correlates simultaneously with the distance to the cluster center ( $T - R$  relation) and with the density of the region where the galaxy is observed ( $T - \Sigma$  relation). The two relations are complementary since in the inner parts of the clusters are also the more dense regions. If the  $T - R$  is the more fundamental relation, as claimed by Whitmore and Gilmore (1991), the morphological segregation would be a global effect, so galaxies would “know” their distances to the cluster center. On the other hand, the  $T - \Sigma$  relation is a local environmental effect, and it would be important even since the epoch of galaxy formation (Dressler, 1980). The presence of the  $T - \Sigma$  and the absence of  $T - R$  relation in poor clusters corroborates with the idea that the local effects are the most fundamental reason for the morphological segregation.

By comparing the galaxy clusters at different redshifts, there is an excess of blue galaxies at higher redshifts compared to lower redshifts, the feature known as Butcher & Oemler effect (Butcher and Oemler, 1984). This result shows that, despite there be no strong evolution in cluster properties, like temperature and intracluster gas metallicity, the galaxies that live in the cluster indeed have evolved in a relatively near past (Lima Neto, 2016).

There is a strong correlation between the SFR and the environmental density, where the densest regions contain galaxies with smallest or none star formation (Hashimoto et al., 1998). The morphological segregation alone is not sufficient to explain this lack of star formation in clusters, as there are observations of passive spirals in high-density regions. These objects can be an intermediate stage between late and early-type galaxies. Infrared observations confirmed the presence of passive spiral galaxies in clusters, against the hypothesis of this galaxies to have hidden star formation, obscured by dust (Yamauchi and Goto, 2004).

Galaxies inside clusters are moving fast, in an environment embedded in hot X-ray emitting gas. If the intracluster medium (ICM) gas pressure is larger than the HI pressure, in outer regions of a galaxy, this cold gas and some stars can be ripped out by ram-pressure stripping. The effect of ram-pressure in galaxies at Coma Cluster is shown in Figure 3.1. This phenomenon is responsible for enriching the ICM since metals are thrown out from galaxies (Gunn and Gott, 1972). The same mechanism is also the cause of strangulation, which is the loss of gas in the halo of galaxies. Under standard conditions, this gas systematically falls in the disk, serving as

fuel to maintain active the star formation. The loss of a significant amount of gas can explain the rapid quenching and the subsequent transformation of spiral galaxies into lenticular inside clusters (Larson et al., 1980).

Tidal effects also act to change the morphology of cluster galaxies. The loss of a non-negligible amount of mass, due to tidal effects, changes the shape of the rotation curve in spiral galaxies inside clusters (Whitmore et al., 1988). High-speed passages or encounter between galaxies through the ICM can heat the galaxy components, increasing its internal energy and making it more vulnerable to disruptions or tidal interactions with other galaxies or with the global cluster potential. This is due to the fact that the typical velocity of galaxies inside clusters (of the order of the cluster's velocity dispersion) is much higher than the galaxy's internal velocity dispersion. The effect of cumulative high-speed encounters, so-called galaxy harassment, can remove substantial mass from the galaxy because the heating pushes stars to unbound orbits.

One interesting characteristic of this phenomenon is that for early-type galaxies, the *de Vaucouleurs* surface brightness profile ( $r^{1/4}$  law) is preserved, even though the harassment can cause substantial mass loss (Aguilar & White, 1986). For late-type galaxies, the disk can be completely destroyed by one or two passages through the cluster, but the central parts still bound (Farouki and Shapiro (1981)). If disk stars remain bound to the galaxy the remnant stars will recover forming a spheroidal system. That can be the history of the dwarf elliptical populations observed in clusters. This effect is more efficient in the more late-type disk galaxies, where the bulge component is less important and the gas is more distributed in outer regions. However, harassment and ram pressure stripping together can transform "early-type disks" (Sa and Sb) into lenticular galaxies.

In general, the probability of galaxies merge inside the massive clusters is relatively low, due to the high velocities involved (Binney and Tremaine, 1987). Nonetheless, the dynamical friction decreases the galaxy's energy and momentum, so it can fall into the cluster's potential well and be "swallowed" by the central galaxy that increases in size and mass. This process is known as Cannibalism and it will happen if the dynamical friction is capable of bringing the satellite galaxy to the center of the cluster within a Hubble time  $1/H(z)$ .

The Cannibalism can occur repeated times, so the central galaxy becomes more and more bright, massive and large. It increases the difference between the luminosity of the first and the second more luminous galaxies in the cluster. This central galaxy eventually also form a big and diffuse envelope, that can be the result of the accretion of material tidally stripped from the cannibalized galaxies (Gallagher and Ostriker, 1972). These galaxies are known as cD galaxies, and they are exclusively found in the center of galaxy clusters.

The "cD" name comes from the *Yerkes galaxy classification scheme*, where "c" refers to the big size, hence supergiant, while "D" refers to the diffuse appearance of its envelope. Several authors (e.g., Ostriker and Tremaine, 1975) believe that these cD galaxies were formed by galactic cannibalism. More recent works showed that the cannibalism model explains well the most of

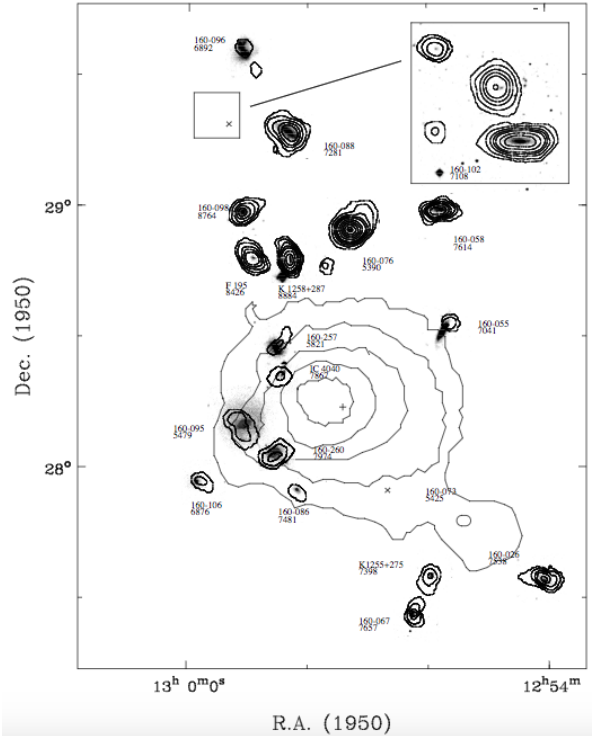


Figure 3.1: The effect of the ram pressure stripping in Coma Cluster. The thick and thin contours represents the X-ray and HI emissions, respectively. The optical image of galaxies are in the background, magnified by a factor of 7. Figure from Bravo-Alfaro et al. (2000).

their properties (e.g., De Lucia and Blaizot, 2007). Central galaxies observed with multiple nuclei are a good evidence that this process really happens. However, observational results suggest that cDs built up most of their mass earlier than the predicted by the cannibalism model (Collins et al., 2009), so this remains an interesting field of study.

## 3.2 Galaxies affect the environment too

It is not clear whether the diffuse light around the cD is part of the galaxy or an intracluster light, that would be stars bound to the cluster potential well, not to any particular galaxy (Mo et al., 2010).

The CDM models predict an efficient gas cooling inside dark matter halos, which would allow the conversion of the hot gas in stars. However, the observations show that a small fraction of the baryons is in stars or cold gas. Some mechanism must prevent the cooling process and the subsequent star formation. The feedback processes are mechanisms where large amounts of energy and material are returned to the surrounding environment, both to the inside or to outside the galaxy. This energy heats the gas and prevents star formation.

Supernovae explosions and AGN jets are examples of feedback processes. The star formation is regulated by the equilibrium between cooling and feedback. A hot gas cloud tends to cool naturally, and the cold gas collapses forming stars. The bigger stars evolve faster and explode as supernovae. The energy delivered in the explosion heats the remaining available gas, suppressing the star formation (negative feedback). On the other hand, the density waves created in the explosion can also compress the gas, inducing an increase of the star formation activity (positive feedback) (see Figure 2.2). Understanding which processes dominate, their details, and how often they occur still are subjects of ongoing studies. Despite massive galaxies are more efficient than the low-mass ones in keeping metals bound during supernova winds, the mechanisms mentioned above, as the ram-pressure and strangulation, are capable of ripping out the gas (containing metals) from the galaxies, thus enriching the environment (Mo et al., 2010).

# Chapter 4

## State of the art

Galaxy evolution is still a promising field of study in astronomy. Despite several authors have already suggested clever ideas to explain the phenomena observed, there still is a lot of disagreements between, not only different interpretations of the same data but also between the observational data *per se*. Details in the observational techniques, technologies, and strategies can lead to different data and consequently different results. Avoiding observational biases is a constant challenge both for the big surveys and for punctual observations done by individual astronomers or small collaboration groups. The methodology used for data analysis is also crucial. For instance, for the same data set, the values of the luminosity function can change significantly, depending on the photometric band used, so it must be taken into account carefully in the interpretation of the results. In addition, there are some disagreements between observations and the predictions made by theoretical or semi-analytic models, as well as measurements with

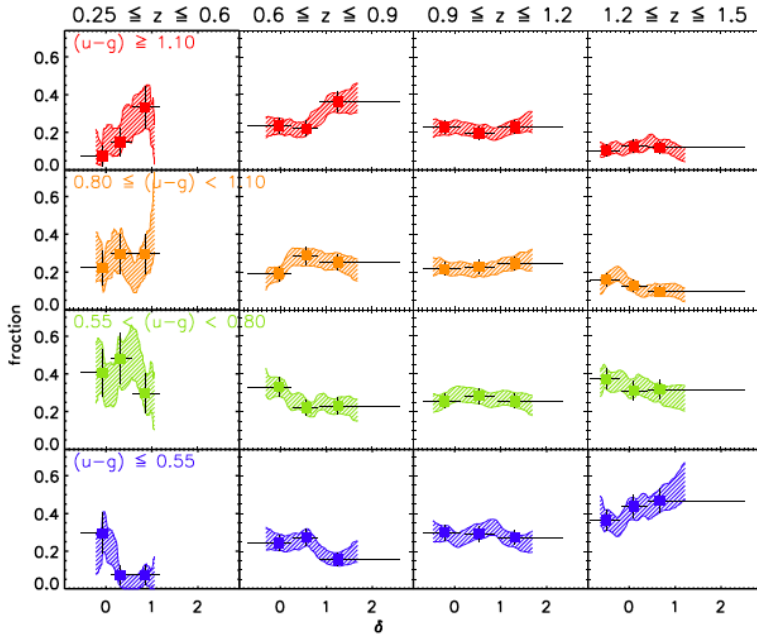


Figure 4.1: Plot from Cucciati et al. (2006), showing color-density relation through the fraction of objects of a given color (in vertical axis) versus the spatial density contrast (in horizontal axis). Rows show the relation for different color ranges, while columns represent different intervals of redshift.

mock data. Therefore, there are a lot of open questions to be answered and another lot of new questions to be done.

This section collects some of the most recent (last  $\sim 15$  years) and relevant findings in this field, aiming to give an overview of what people have been working on. Due to the limited size of this text, I do not intend to cover all the topics existing in the literature. Instead, I choose, purposely, some of the most interesting works that explore directly or indirectly the relationship between the evolution of the galaxies and the environment where they live, all of them based on observational data. These works will be presented in the chronological order, with no compromise to keep a homogeneous level of details between them.

In 2001, Balogh et al. investigated the dependence of the galaxy infrared LF and the associated stellar MF on the environment and spectral type, using photometric data from Two Micron All-Sky Survey (2MASS) (J and  $K_s$  bands) and spectroscopic redshifts from Las Campanas Redshift Survey (LCRS, local Universe,  $z < 0.2$ ). The spectral classification was based on emission-line and non-emission-line galaxies, representing star-forming and quiescent galaxies. For environmental classification, they used a “friends-of-friends” algorithm to search for overdensities and to calculate velocity dispersion ( $\sigma_1$ ) of cluster candidates. Clusters were defined as the overdense regions where  $\sigma_1 > 400 \text{ km s}^{-1}$ . Groups were defined as the cluster candidates with  $\sigma_1 < 400 \text{ km s}^{-1}$ . By elimination, the field was set as the rest of galaxies out of the overdense regions. The  $D_{4000}$  spectral indexes from the LCRS spectra were used to determine stellar masses, needed to calculate the stellar MF.

Balogh et al. (2001) found that, in the field, the LF for star-forming galaxies have much steeper faint-end slopes than that for quiescent ones. In clusters, both galaxy types have LFs with a steep faint-end. The overall LF and MF are significantly different in clusters and field environments, with a brighter characteristic magnitude ( $M^*$ ) and a steeper faint-end slope ( $\alpha$ ) in clusters. Based on these results, they conclude that in lower density environments, the faint population is dominated by star-forming galaxies. In clusters, regular galaxies are, in average, brighter than in the field (brighter  $M^*$ ). They also found that the MF shape for quiescent galaxies in clusters is similar to the total MF shape in the field. This similarity would be due to the fact that field galaxies are the building blocks for the formation of clusters. Galaxy clusters are mostly built up of (ex-)field star-forming galaxies, in which star formation has quenched because either the galaxies consumed all their gas, by formed earlier (because of their proximity to a large mass perturbation) or by external environmental gas loss, e.g. through processes like ram pressure

stripping or strangulation.

In 2003, Kodama & Bower studied the LF and MF in three clusters at higher redshifts ( $z \sim 1$ ), using near-infrared imaging data from the 4.2 m William Herschel Telescope at La Palma. They found an LF shape very similar to lower  $z$  counterparts such as that from 2MASS/LCRS clusters given by Balogh et al. (2001). This indicates a little evolution of galaxy masses since  $z = 1$  in these dense environments. There is pure luminosity evolution, with constant stellar mass, according to the passive evolution since then.

The comparison with predictions from semi-analytic hierarchical galaxy formation models shows incompatibilities. The models predict the increase of characteristic mass by more than a factor of  $\sim 3$  since  $z = 1$  to the present day. The fraction of giant galaxies at  $z = 1$  in the semi-analytic predictions is a factor of 3 smaller than the observed value. Massive galaxies ( $> 10^{11} M_{\odot}$ ) correspond to a large fraction of the galaxy population at this  $z$ , which disagrees with the predictions of current hierarchical galaxy formation models. Both star formation and mass assembly were strongly accelerated in clusters. It was completed in clusters at  $z = 1$  and even earlier ( $z \gg 1$ ) in the cluster core. The reason for the lack of mass growth in clusters at lower redshifts may be due to the fact that galaxy-galaxy mergers are likely to be less effective in the higher density environment. The velocities in a cluster core are too high to allow galaxy encounters (Binney and Tremaine, 1987).

After a couple years, Cucciati et al. (2006) analyzed  $\sim 6.5$  k galaxies with good quality spectroscopic redshifts from VVDS, up to  $z \sim 1.5$ , to study the build-up of the color-density relation over time. Spatial densities were quantified in relatively local scales (radius of  $5 h^{-1}$  Mpc). Three environments were defined, basically considering the spatial density above, below, or equal to the average global density (corresponding to the three points in the each panel of Figure 4.1). They found that the color-density relation strongly depends on the redshift. At low  $z$  there is a steeper color-density relation, where the fraction of the reddest galaxies increases with spatial density. The opposite is observed for the bluest galaxies and no strong dependence is detected for intermediate colors (flat relation). This trends weaken with increasing redshift, disappearing at  $z \sim 1.5$  (see Figure 4.1, that shows this relation for a subsample of bright galaxies.)

The first column in Figure 4.2 shows that the bimodality in the color-magnitude space, known in the local Universe, is already well defined at higher redshifts ( $z \sim 1.5$ ). The second and

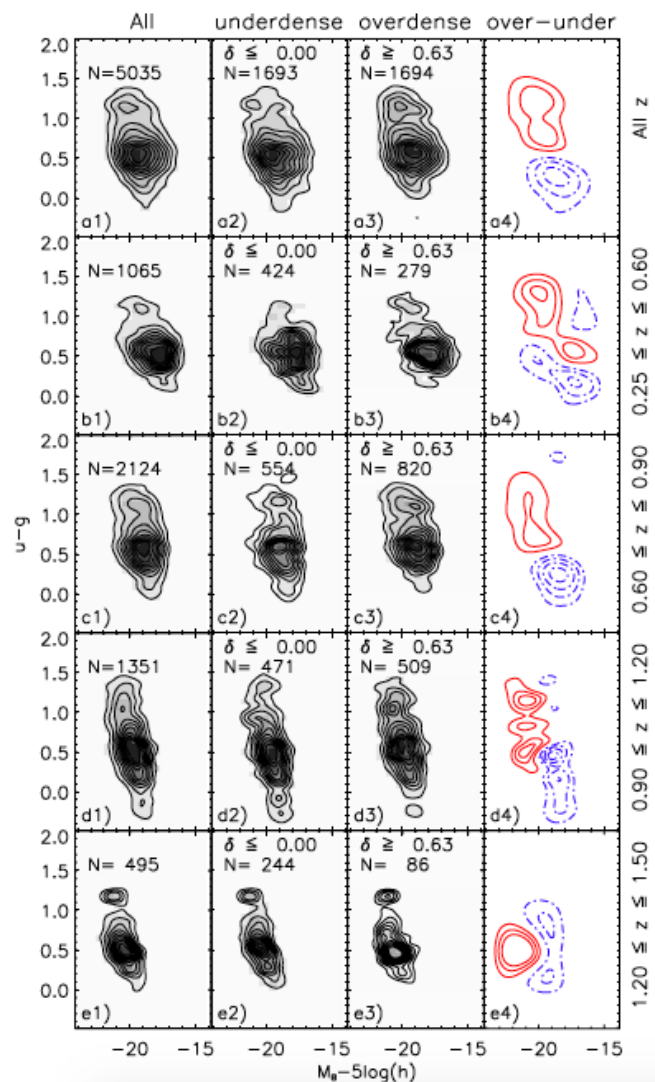


Figure 4.2: Plot from Cucciati et al. (2006), showing isodensity contours in the  $(u^* - g)$  vs.  $(M_B - 5 \log h)$  CMD for different redshift ranges (rows) and environments (columns).  $N$  is the number of galaxies in each bin. The gray scale is normalized, for each panel, to the total number of objects contained in that panel. The last column shows the difference between the overdense and underdense environments' colour-magnitude distributions. The curves correspond to 1, 2, and  $3\sigma$  levels of significance in the differences. Positive differences are shown in red and negative differences in blue.

intermediate colors (flat relation). This trends weaken with increasing redshift, disappearing at  $z \sim 1.5$  (see Figure 4.1, that shows this relation for a subsample of bright galaxies.)

third columns show that this bimodality survives irrespective of the environment in all redshift range studied. The fourth column shows that the colour-magnitude distribution depends on the environment. At higher  $z$ , overdense regions were mostly populated by bright blue objects. Even the brightest red galaxies are not preferentially found in these regions. At  $0.9 < z < 1.2$ , the red objects become more likely to be found in overdense regions, and this trend remains up to  $z = 0$ . In this bin, they tend to be brighter than bluer objects that are more present in lower density regions. At low redshift, red objects still more likely to be found in overdense environments, but there it is true for any luminosity.

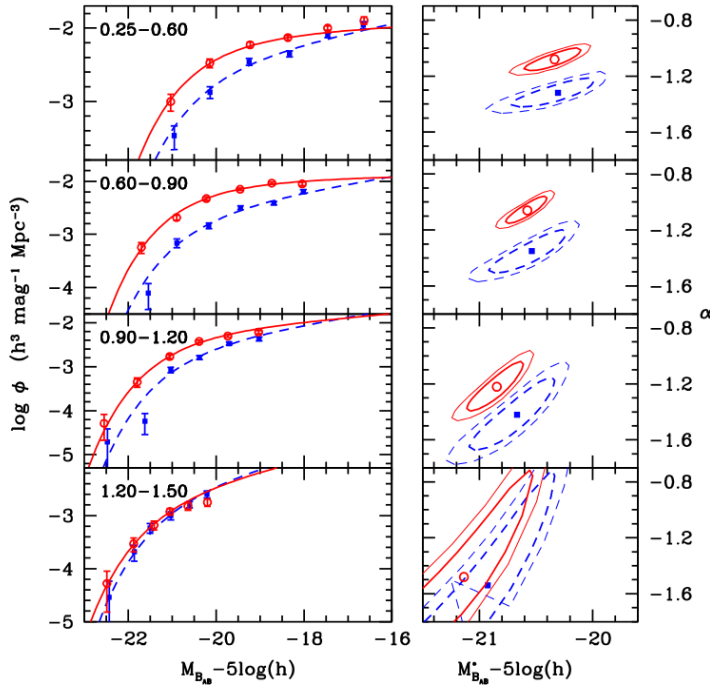


Figure 4.3: Plot from Ilbert et al. (2006b). Left panels show the B-band LF for underdense (blue) and overdense (red) environment. The lines correspond to LFs fitted to single Schechter functions. The points correspond to the non-parametric estimate obtained with the  $1/V_{max}$  method. Right panels:  $M_B - 5 \log(h)$  vs.  $\log \phi^*$  with the corresponding 68% (thick lines) and 90% (thin lines) error contours obtained with the STY estimator. Redshift range increases from top-down.

environment definition was done based on the density contrast ( $\delta$ ), determined by using a Gaussian filter of smoothing length  $5h^{-1}$  Mpc to reconstruct the 3D galaxy density map, then comparing local densities with the global average.

The results obtained by Ilbert et al. (2006b) showed that for  $z \leq 1.2$ , the LF shape is strongly dependent on the large-scale environment (see Figure 4.3), although  $M^*$  is continuously dimming from  $z = 1.5$  to  $z = 0.25$  for the two environments defined. Underdense regions present an LF with a steeper faint-end slope. The high-mass end is dominated by galaxies living in overdense environments, for  $z < 1.2$ . For  $1.2 \leq z \leq 1.5$  both environments show similar LFs, considering the uncertainties. They claimed that the LF shape is imprinted very early in Universe. The physical processes shaping up the environment relation have already been efficient earlier than the redshift range considered in this study.

The evolution of the luminosity density ( $\rho_L$ ) in the B-band rest frame is also dependent on the environment, as shown in Figure 4.4. In underdense regions, the luminosity density is continuously decreasing with comic time (in the redshift interval studied), a consequence of the fading of  $M^*$ . This result could be explained by the continuous decrease of the SFR in

The evolution of both color-density and color-magnitude-density relations are supposed to be the product of internal and external factors that have been occurring over a period of at least 9 Gyr. These results are in agreement with an evolutionary scenario where the processes happen in shorter time scales for the high-mass objects and in the highest density environment. There was an epoch, earlier for the most massive galaxies when the colour-density relation began to be significant on the  $5h^{-1}$  Mpc scales. The star formation ends at earlier epochs for more luminous/massive galaxies and it continues to be substantial at the present day in field galaxies, especially for the fainter objects.

In 2006, Ilbert et al. (2006b) studied the dependence of the LF on the environment, using  $\sim 6.5$  k galaxies with measured spectroscopic redshifts, also in the range  $0 \leq z \leq 1.5$ , from the VVDS first epoch data. The LF was calculated using two different methods separately in four redshift intervals and two (underdense and overdense) environments. The

environment definition was done based on the density contrast ( $\delta$ ), determined by using a Gaussian filter of smoothing length  $5h^{-1}$  Mpc to reconstruct the 3D galaxy density map, then comparing local densities with the global average.

The results obtained by Ilbert et al. (2006b) showed that for  $z \leq 1.2$ , the LF shape is strongly dependent on the large-scale environment (see Figure 4.3), although  $M^*$  is continuously dimming from  $z = 1.5$  to  $z = 0.25$  for the two environments defined. Underdense regions present an LF with a steeper faint-end slope. The high-mass end is dominated by galaxies living in overdense environments, for  $z < 1.2$ . For  $1.2 \leq z \leq 1.5$  both environments show similar LFs, considering the uncertainties. They claimed that the LF shape is imprinted very early in Universe. The physical processes shaping up the environment relation have already been efficient earlier than the redshift range considered in this study.

The evolution of the luminosity density ( $\rho_L$ ) in the B-band rest frame is also dependent on the environment, as shown in Figure 4.4. In underdense regions, the luminosity density is continuously decreasing with comic time (in the redshift interval studied), a consequence of the fading of  $M^*$ . This result could be explained by the continuous decrease of the SFR in

these objects. Galaxies in such environment are supposed to passively evolve isolated, just consuming the internal gas present in their halos. On the other hand, in overdense regions, the increase of the characteristic normalization ( $\phi^*$ ) compensates the decrease of  $M^*$ , causing the increase of the luminosity density in the range  $0.25 < z < 0.9$ . Since the galaxies become more clustered over the cosmic time, as modeled by the hierarchical scenario, the fraction of objects in overdense environment tends to increase. The combination of this hierarchical growth of large-scale structures the decreasing in the SFR could explain the peak of the luminosity density in overdense environments at  $z \sim 0.9$ . Environmental mechanisms like ram-pressure stripping, harassment and strangulation could speed up the star formation quenching in infalling galaxies, contributing to the increase of faint red galaxies over time.

In 2007, Faber et al. (2007) published a remarkable paper that did not address directly the environmental effects on galaxy evolution but introduced a new perspective on the mechanisms responsible for the migration of galaxies from the blue cloud to the red sequence in the CMD. They used a sample of 39 k galaxies from the combination of two surveys, with spectroscopic redshifts ( $\text{spec-}z$ ) from DEEP2 and “high resolution” (17 bands) photometric redshifts ( $\text{photo-}z$ ) from COMBO-17, to calculate the LF for blue and red galaxies, separately, fitted to single Schechter functions, assuming constant  $\alpha$ .

They observed that the total sample becomes fainter with time for the redshift range considered ( $z \leq 1.2$ ), evident by the dimming in the global characteristic absolute magnitude  $M_B^*$ , but they still virtually constant in number density (see Figure 4.3). The population of blue galaxies follows the same trends of the global LF, which is expected since the whole sample is dominated in number by blue galaxies. The luminosity density  $j_B$  decreases with time for blue galaxies, consistent with passive evolution. The red population is increasing in number density with time and its  $M^*$  is dimming since  $z \sim 1.2$ , but the luminosity density has remained roughly constant. The rise in the number of red galaxies applies to galaxies near  $M^*$ , not for much more luminous galaxies.

The number and stellar mass of blue galaxies show no substantial evolution since  $z \sim 1$ . On the other hand, the number of red galaxies is increasing at this epoch. The appearance of new red galaxies is explained through a “mixed” scenario, where galaxies migrate from the blue cloud to the red sequence because of the quenching of their star formation activity, mainly due to wet, gas-rich mergers (the CMD schema is shown in Figure 4.5). Once in the red sequence, they continue to merge (now mainly via dry, stellar mergers), building up the most massive red galaxies. The dominant mechanism responsible for driving blue galaxies to the red sequence depends on the epoch and the characteristic mass. The red sequence would be constructed in variate ways at different times and masses. So it would be a complex process, not possible to be explained by a single process of “downsizing” or “upsizing”.

In 2007, Gerke et al. used DEEP2 galaxies in the redshift range  $0.75 \leq z \leq 1.3$  to determine the role of the galaxy groups in driving the color evolution at high  $z$ . They found that the fraction of blue galaxies in groups is significantly lower than in the field, for the range,  $0.75 \leq z \leq 1$ .

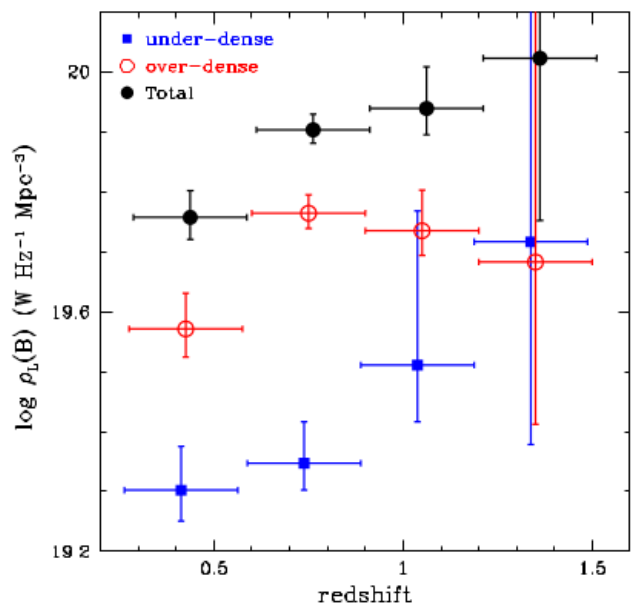


Figure 4.4: Plot from Ilbert et al. (2006b): the evolution of the luminosity density ( $\rho_L$ ) in the B band as a function of redshift. Open red points refer to the overdense environment, solid blue squares to the underdense environment and solid black circles to the total sample.

The number and stellar mass of blue galaxies show no substantial evolution since  $z \sim 1$ . On the other hand, the number of red galaxies is increasing at this epoch. The appearance of new red galaxies is explained through a “mixed” scenario, where galaxies migrate from the blue cloud to the red sequence because of the quenching of their star formation activity, mainly due to wet, gas-rich mergers (the CMD schema is shown in Figure 4.5). Once in the red sequence, they continue to merge (now mainly via dry, stellar mergers), building up the most massive red galaxies. The dominant mechanism responsible for driving blue galaxies to the red sequence depends on the epoch and the characteristic mass. The red sequence would be constructed in variate ways at different times and masses. So it would be a complex process, not possible to be explained by a single process of “downsizing” or “upsizing”.

In 2007, Gerke et al. used DEEP2 galaxies in the redshift range  $0.75 \leq z \leq 1.3$  to determine the role of the galaxy groups in driving the color evolution at high  $z$ . They found that the fraction of blue galaxies in groups is significantly lower than in the field, for the range,  $0.75 \leq z \leq 1$ .

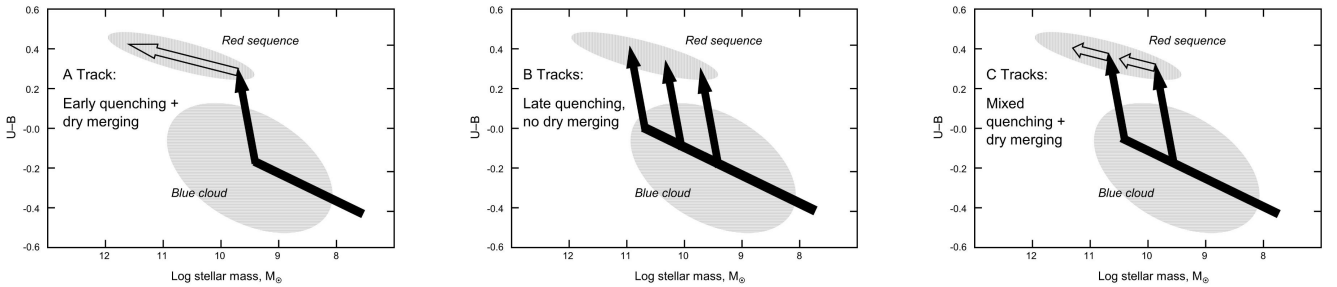


Figure 4.5: Diagrams from Faber et al. (2007). The first two panels shows different hypothesis for the build-up of the red sequence. It is assumed that red galaxies arise from blue galaxies via wet (gas rich) major ( $\sim$ doubling the mass) mergers (black arrows). In the first scenario, galaxies would migrate with lower masses, and undergo subsequent dry mergers, populating the high mass end of the red sequence. In the second scenario, galaxies would undergo wet major mergers having different masses, so all the horizontal extension of the red sequence in CMD could be filled without the need of dry mergers. The last scenario, proposed by the authors as the more realistic between the three presented, would be a combination of the previous two, with contributions from both mechanisms.

The well-known color segregation is already in place at  $z \sim 1$  and is correlated with the amount of galaxy members in the groups: the richer the group, the lower the fraction of blue galaxies. The luminosity is also related to color: fainter galaxies are more likely to be blue, independently of the environment. The fraction of blue galaxies in groups decreases drastically with decreasing redshift from  $z = 1.3$  to  $z = 1$ , while there is no significant evolution over the range  $0.75 \leq z \leq 1$ . At  $z \sim 1.3$ , the fractions of blue galaxies in groups and in the field become indistinguishable, as it is evident in Figure 4.6.

The evolution in the fraction of blue galaxies, that weakens at  $z \lesssim 1$ , is different in nature from the classical Butcher-Oelmer effect, where the fraction of blue galaxies in galaxy clusters reduces from  $z \sim 0.5$  up to the present days. The last is a natural outcome of the hierarchical structure formation, provided that at this range, clusters and groups are already efficient in quenching the star formation of the galaxies that falls into them. The convergence between the fractions of blue galaxies in groups and in the field at  $z \sim 1.3$  implies that, at some epoch, groups were not so efficient in quenching the infalling galaxies.

Semi-analytic models of galaxy formation (Gerke et al. quotes: Bower 2006; Cattaneo et al. 2006; Croton et al. 2006; Kang et al. 2006) state that galaxies are quenched when they reach a halo mass threshold of a few times  $10^{12} M_\odot$ , that is large enough to strengthen AGN activity in a level that the feedback stops gas cooling and condensing to form stars. The DEEP2 galaxy groups studied have masses in the range of  $5 \times 10^{12}$  to  $5 \times 10^{13} M_\odot$ . According to these models, a typical halo in this mass range at  $z \sim 1.3$  would reach threshold mass for quenching around  $z \sim 2$ . Hence, supposing that a quenched galaxy takes  $\sim 1$  Gyr to migrate from the blue cloud to the red sequence, the galaxy groups would become a suitable environment for quenching at  $z \sim 2$ .

Zucca et al., in 2009, used photometric data in the COSMOS field (10 bands from different surveys), combined with spectroscopic redshifts from the zCOSMOS 10 k sample and HST images to study the role of the environment in the evolution of the B-band LF of different galaxy types. The types were classified using two different criteria: (a) morphological types was assigned by a Nearest Neighbor training-based algorithm, from structural parameters measured in the HST images, using a training sample with  $\sim 500$  galaxies for which eye-ball morphological classification is available. The morphological groups defined were: early-types (E+S0), spirals and irregulars; (b) spectrophotometric types were assigned via template fitting, using the same SED templates as used by Ilbert et al. (2006b). The groups were defined based on the colors obtained from the best-fit SED, so the galaxies were divided into type 1 (E+S0), type 2 (early spirals), type 3 (late spirals), type 4 (irregulars + starbursts).

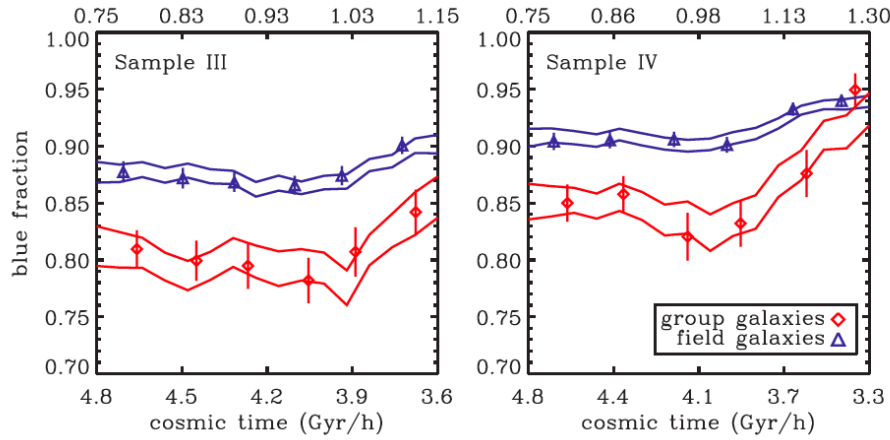


Figure 4.6: Plots from Gerke et al. (2007): evolution of the fraction of blue galaxies in two of the four samples studied in the paper.

The two classifications resulted in marginally different fractions of early and late-types, mainly for the fainter objects. Some galaxies classified as “red spirals” by the spectrophotometric classification, after visual inspection, were revealed to be spiral galaxies very affected by dust extinction. Besides that, some of the morphological early-types were considered late-type by the spectrum (color) analysis. These “blue early-types” were also visually inspected, revealing a group of face-on late-type galaxies with morphological parameters typical early-type objects.

Environments were defined based on the fifth nearest neighbor, the same described in Bolzonella et al. (2010) (this paper was published first, but at the time, Zucca et al. (2009) cited the Bolzonella et al. (2010)’s draft, that was available in arXiv). Galaxies were divided into four quartiles of overdensity. The LF was computed for the first and the fourth quartiles, to compare respectively the underdense and the overdense regions. An important caveat is that when comparing the LF between environments, only the comparison between LF shapes or the evolutionary trends makes sense. The numerical value of the normalization  $\phi^*$  is affected because this kind of selection does not conserve information about the volume occupied by the overdensity associated to each galaxy.

The results obtained indicated that the global LF (for all environments and galaxy types together) show a dimming in  $M^*$  with cosmic time, which is in agreement with previous results using VVDS data for similar redshift ranges, and with previous paper mentioned above (e.g., Ilbert et al., 2006b; Faber et al., 2007).

Considering all environments, both separating galaxies by spectrophotometric types and morphological types, at lower  $z$ , late-types dominate the LF faint end, while early-types dominate the bright end. The contribution to the LF bright end at  $z \sim 1$  of the various types is comparable, while the faint end remains dominated late-type galaxies. Early-type evolves in both luminosity and normalization:  $M^*$  becomes fainter, and  $\phi^*$  increases with the cosmic time, in agreement with the red sample in Faber et al. (2007). Late-type also becomes fainter, but  $\phi^*$  decreases with time ( $\phi^*$  for blue galaxies was virtually constant with time in Faber et al. (2007)). Intermediate types show a milder evolution of  $M^*$  and no significant evolution in  $\phi^*$ .

Studying separately the galaxies in the two extreme environments, for all galaxy types, the LF in overdense regions has always a brighter  $M^*$  and a flatter slope, in agreement with Ilbert et al. (2006b), as shown in the left column of Figure 4.7. The crossing points between the two LFs, in underdense and overdense environments, moves progressively towards fainter magnitudes with decreasing redshifts (comparing the 3 panels in the first column of Figure 4.7).

As well as for the total sample,  $M^*$  is always brighter in overdense regions, even for the galaxy types separately. The differences between the global LF in the two environments are not only due to a difference in the relative number of early and late-types but also to their relative luminosity distributions. Although the large uncertainties in the faint end, it is very clear the contrast between  $\alpha$  from types 1 and 3+4.

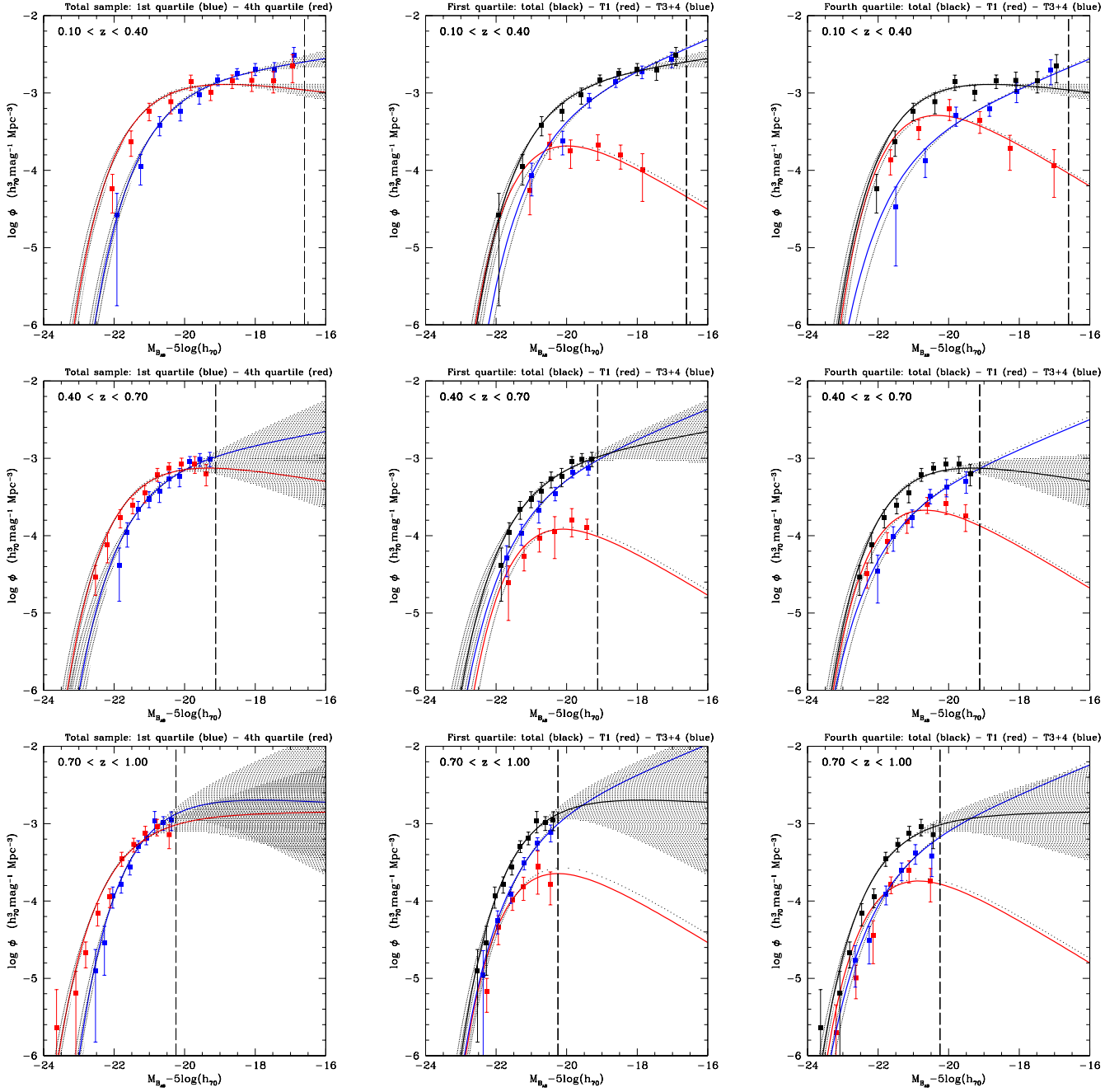


Figure 4.7: Plots from Zucca et al. (2009): LF in 3 redshift bins, 2 environments and 2 spectral types, separately. In the left column: LF in the lowest (blue) and highest (red) quartiles of density, for all spectral types together. Middle and right columns shows the LFs in the lowest and highest density quartiles, respectively, for the type 1 (ellipticals and S0s, in blue), types 3+4 (late spirals, irregulars and starbursts), and the total sample (all spectral types, in black). The shaded regions represent the 68% uncertainties on  $\alpha$  and  $M^*$ . For the cases where  $\alpha$  is fixed, the shaded area is not drawn.

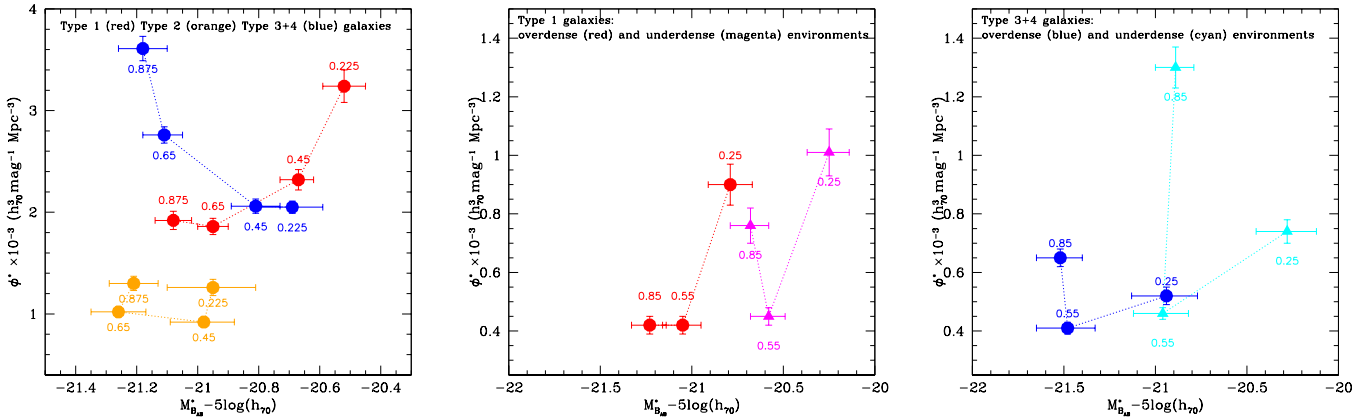


Figure 4.8: Plots from Zucca et al. (2009): evolution of the  $M^*$  and  $\phi^*$  (derived with  $\alpha$  fixed) for different samples (the redshift bin center is indicated next to each point). Left panel: all environments and spectral types. Early-types (middle panel) and late-types (right panel) are show separately for the two extreme environments.

For all the environments, the  $M^*$  is becoming fainter with time for both early and late-types, consistent with passive evolution, while intermediate types virtually have no evolution (see left panel of Figure 4.8). However, the opposite evolution of  $\phi^*$  for early and late-types favors a scenario where a part of late-type is transformed into early-types with increasing cosmic time, without significant changes in the fraction of intermediate-type galaxies.

Regarding the two extreme environments, early-type (middle panel of Figure 4.8) and late-type galaxies (right panel of Figure 4.8) shows an evolution in overdense environments consistent that for the total sample. In underdense environments, the same is true, except for the highest redshift bin, where early-types show a strong increase in the normalization comparing to the intermediate redshift bin. The clear difference in late-type galaxies LF evolution in different environments, with a much stronger density evolution in underdense regions, indicates that most of the transformation from blue to red galaxies in overdense regions probably happened before  $z \sim 1$ , not being accessible with these data set, while it is still ongoing at lower redshifts in underdense environments.

In 2010, Bolzonella et al. used a similar data set to study the impact of the environment in the galaxy evolution. They also used data from zCOSMOS survey, in the redshift range  $0.1 \leq z \leq 1.0$  combined with multiwave-length photometry, over an area of  $\sim 1.5 \text{ deg}^2$ . That paper, stellar masses were estimated via SED fitting, using a mix of theoretical SED templates from three different models of stellar population synthesis. Morphological types were also determined via SED fitting, but using observed SEDs as templates together with interpolated SEDs, to enrich the primary set of observed ones.

The stellar MF was computed using the  $1/V_{max}$  method, and fitted to both single and double Schechter functions. Environments were classified using spec-zs, that are more accurate than

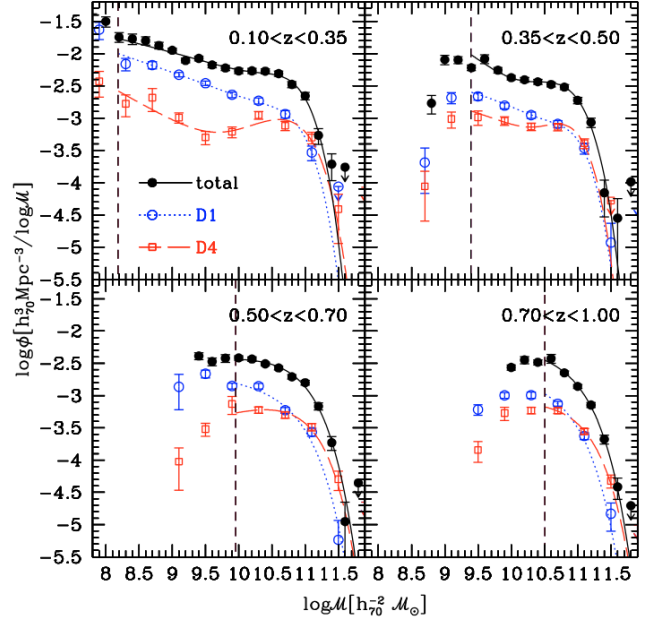


Figure 4.9: Plots from Bolzonella et al. (2010): the MFs in the extreme quartiles of environmental density D1 (lower overdensities, in blue) and D4 (higher overdensities, in red). In black the MF for the total sample.

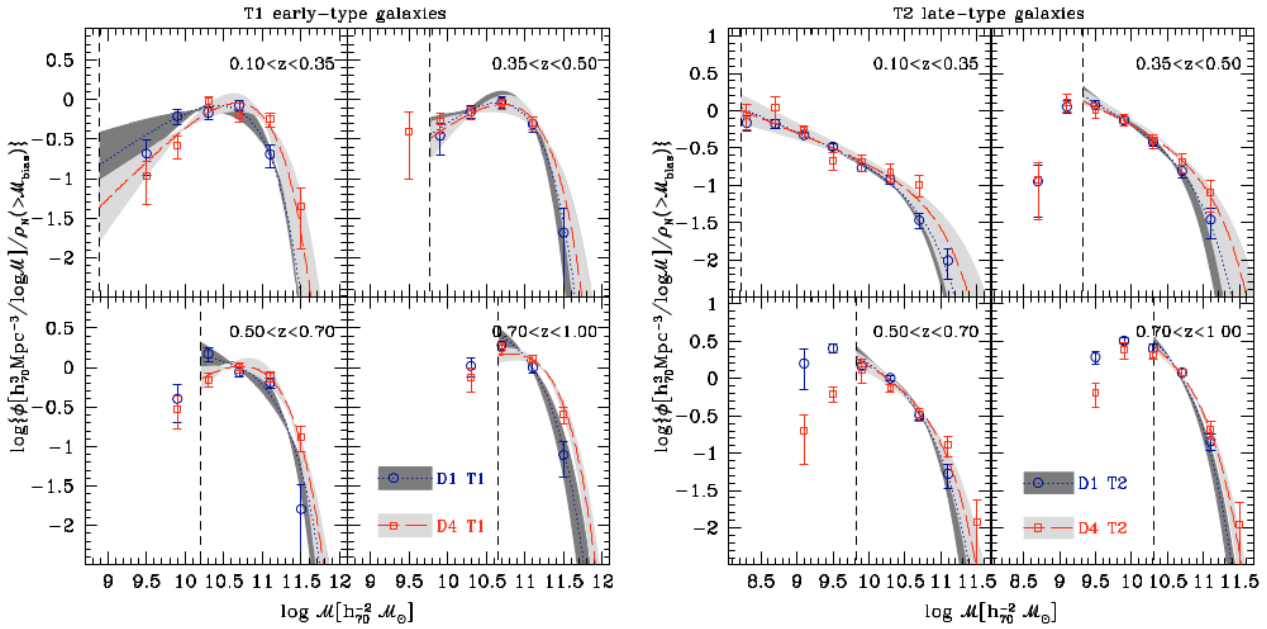


Figure 4.10: Plots from Bolzonella et al. (2010): MFs of early-type galaxies (left panel) and late-type galaxies (right panel), for lower density (in blue) and higher density (in red) environments.

photo-zs, to delineate a skeleton of large scale structures. The local density contrast ( $\delta$ ), a function of RA, Dec, and redshift, were then computed by counting objects in the photo-z sample, that is less affected by the incompleteness of faint objects, within a radius that includes up to the fifth nearest neighbor in the spec-z sample. The sample was divided into four quartiles of overdensity ( $1 + \delta$ ), and the two extreme quartiles, D1 and D4, were compared.

At low  $z$ , the MF is extremely different in high- and low-density environments. Low mass galaxies are preferably found in lower density environments, as shown in Figure 4.9. The MF for the higher density environments shows a marked bimodality, not reproducible by a single Schechter function. This bimodality is interpreted to be due to the contributions of different morphological types. These differences become less important with increasing redshift, being negligible at  $z \sim 1$ , although the limiting magnitude of the survey (dashed vertical line in Figure 4.9) make it difficult to conclude.

The shapes of the MFs and its evolution for different morphological types, separately, are almost identical for the extreme environments considered, evident in Figure 4.10. Therefore the differences in the global MFs in the two extreme environments are due to the evolution of the normalization ( $\phi^*$ ) of these functions.

By comparing the MFs for early and late-type galaxies in different environments, the increase in early-type galaxies with cosmic time could be explained by blue intermediate-mass galaxies being transformed into more massive red galaxies, after quenching star formation, more efficiently in overdense than in underdense regions. This difference in efficiency reflects in different time scales for the transformations, which is possible to quantify, for instance, by considering the  $M_{cross}$ : the mass above which the MF is dominated by early-type galaxies. Figure 4.11 shows that at  $z \sim 1$  the  $M_{cross}$  values were very similar in low and high density environments. As galaxies evolve, the difference between the two  $M_{cross}$  values becomes significant. The ratio between values in the highest to lowest redshift bins implies an evolution in high-density more than twice larger than in low density. In other words, “the environment begins to affect the evolution of galaxies at  $z \sim 1$ , causing in the lowest redshift bin a delay of  $\sim 2$  Gyr in underdense relative to overdense regions before the same mix of galaxy types is observed in high-density regions.”

Bolzonella et al. (2010) also found that the speed of evolution is different for distinct morphological groups. It suggests that the migration from the blue cloud to the red sequence occurs more quickly than the transformation of disks into ellipticals.

Finally, they conclude that galaxy evolution depends on both the stellar mass and the environment. These two factors are inseparable since the environment set the probability of a galaxy to have a given mass. Environmental mechanisms start to be more effective at  $z < 1$ . They also compared their results with those obtained with mock catalogs based on semi-analytic models, finding disagreements in both low and high-density environments. They argue that, for the sparse environments, the models does not properly account for the star formation suppression, leading to an over-prediction of the amount of blue. For the densest regions, models predict an excess of red galaxies at  $z < 0.5$ , because of the over quenching of satellites.

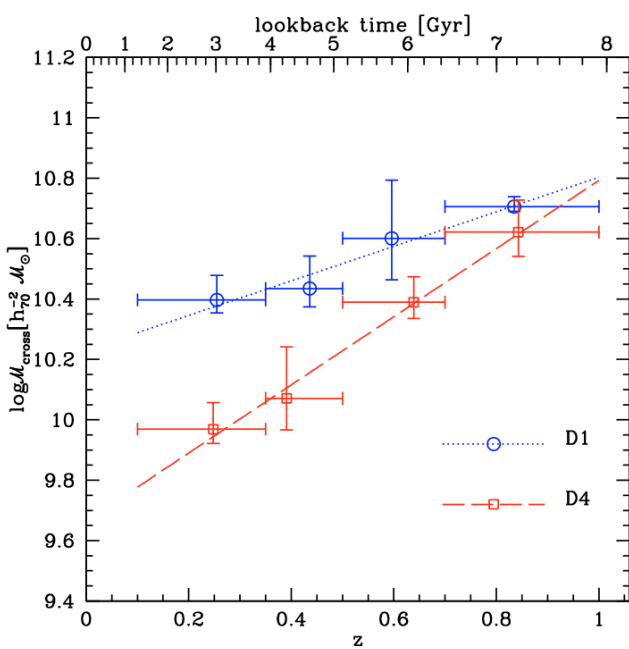


Figure 4.11: Plots from Bolzonella et al. (2010):  $\mathcal{M}_{\text{cross}}$  of photometric types in the extreme quartiles D1 (low-density, in blue) and D4 (high-density, in red).

a large area, which is useful to measure environments. This sample contains more than 100 k objects with reliable redshifts, stellar masses and rest-frame colors (via SED fitting). The second and third samples were used to access the low-mass regime. CANDELS UDS and CANDELS GOODS-S covers a small area, but have high resolution, which is useful for exploring galaxy morphological structures. CANDELS UDS is 3.5 magnitudes deeper than UDS, in H-band, and CANDELS GOODS-S has a large spectral coverage, 17 bands from UV to IR. The data from different sources was homogenized to serve as a unique dataset. Redshifts, stellar masses, and rest-frame colors were obtained via SED fitting, with synthetic SEDs constructed from Bruzual & Charlot (2013).

For each data set, the MF was computed for the entire sample and split by colors, structural parameters, and environments. They explored the links between environmental overdensity, morphology, and the quenching of star formation. To do that, galaxies were separated by three different criteria: (1) Colors: red and blue, representing passive and star-forming galaxies, based on rest-frame U-V and V-J colors combined, in addition to other redshift dependent criteria. A little amount of dusty star-forming galaxies is expected to contaminate the passive galaxy sample. (2) Environments: densities were quantified by counts in a physical aperture, a cylinder around each galaxy. The high-density environment is where density is  $> 1\sigma$  above the mean density (in

In 2015, Mortlock et al. explored the MF evolution of galaxy populations with respect to color, environment, and structure, to understand better how galaxy evolution depends on these 3 factors, separately. They defined three samples: the first used photometric data from the Ultra Deep Survey (UDS), the second combined this data with data from the Cosmic Assembly Near-infrared Deep Extragalactic Legacy Survey (CANDELS), and finally the third combined CANDELS data with data from the Great Observatories Origins Deep Survey-South (GOODS-S). That is UDS, CANDELS UDS, and CANDELS GOODS-S, covering  $0.88 \text{ deg}^2$ , with redshifts from 0.0 to 3.0 (a considerable advance in redshift range covered, compared to the previous works mentioned here).

The first sample was used to study the regime of high-mass galaxies. UDS covers

, despite being shallower than the other

the redshift bin considered). Low-density is where it is  $< 1\sigma$  below the mean. (3) Morphological structure (two classifications): 3a) Sérsic index — two populations:  $n >$  or  $< 2.5$ , representing the light more centered or more spread in the galaxy surface, respectively. 3b) Concentration, asymmetry and clumpiness (CAS) parameters, as an indicator of high/low asymmetry in the galaxy shape.

They parametrized the MF with single or double Schechter functions, according to convenience (they tried both and choose the fit with smaller  $\chi^2$  for each case). For instance, for the global MF, they used double Schechter function to for lower redshift bins ( $0.3 < z < 1$ ) and single Schechter for the rest ( $1 < z < 3$ ). They found that  $\phi^*$  increases with cosmic time. It is observed a flattening of  $\alpha$  from low to intermediate redshifts ( $0.3 < z < 1.5$ ), and a steepening from intermediate to high- $z$  ( $1.5 < z < 3$ ). The characteristic mass ( $M^*$ ) is nearly constant from  $z = 0.3$  up to  $z = 3$ . They compared with previous results in the literature, and found a good agreement in the behavior of the Schechter parameters, except for those works that impose a fixed value for  $\alpha$ .

The evolution of the Schechter parameters  $\phi^*$ ,  $M^*$  and  $\alpha$  can be interpreted as the evolution in mass for the total, high-mass, and low-mass galaxy populations, respectively.  $\phi^*$  is expected to increase from high to low redshifts since the galaxies are constantly growing in stellar mass (a classical result widely present in the literature, consistent with the hierarchical scenario). The MF faint-end is steeper at higher redshifts, showing that low stellar mass galaxies contributed significantly to the total stellar mass budget in the earlier Universe. The flattening of  $\alpha$  can be explained by the increase of stellar mass in lower mass galaxies, for instance, via merging or gas accretion.  $M^*$  does not show strong evolution in such redshift range. Although the density of massive galaxies is increasing over time ( $\phi^*$  goes down with redshift), the typical stellar masses around the MF knee are not strongly evolving. This result is consistent with the downsizing (Cowie et al., 1996) phenomenon, where the most massive galaxies build up their mass first.

The results for the morphological types based on CAS parameters shows that the evolution of the low asymmetry MF is very similar to the evolution of the global MF because the asymmetric population contributes very little to the total mass budget in this redshift range. Galaxies with low asymmetry dominate at all ranges of masses and redshift studied in this work. The MFs for symmetric and asymmetric galaxies are roughly similar in shape for all redshift bins studied, differing mostly in the normalization.

The comparison between the global MF and that for blue and red galaxies separately showed a clear dependence between mass and color. The MF high mass end is dominated by red galaxies, while the low-mass end is dominated by blue galaxies. This dependence becomes stronger with decreasing redshift. It is evident in Figure 4.12 that the increase in the total mass is driven by the rapid growth of the quiescent galaxy population, that becomes dominant (in stellar mass density) at  $z \sim 2$ , while the star-forming population remains almost constant in the redshift

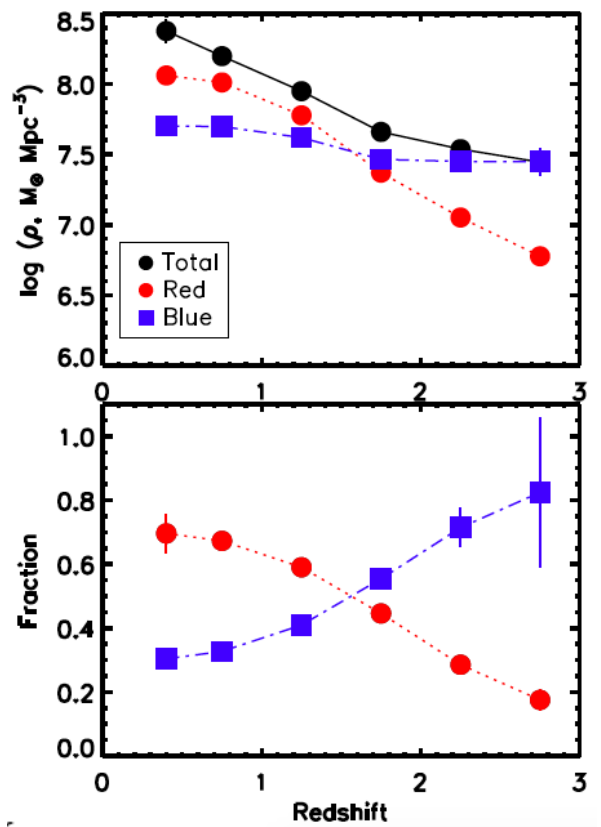


Figure 4.12: Plots from Mortlock et al. (2015). Top panel: stellar mass density versus redshift for star-forming (blue), quiescent (red), and for the total sample (black). Bottom panel: the fraction of stellar mass density fro the total.

asymmetry galaxies are roughly similar in shape for all redshift bins studied, differing mostly in the normalization.

The comparison between the global MF and that for blue and red galaxies separately showed a clear dependence between mass and color. The MF high mass end is dominated by red galaxies, while the low-mass end is dominated by blue galaxies. This dependence becomes stronger with decreasing redshift. It is evident in Figure 4.12 that the increase in the total mass is driven by the rapid growth of the quiescent galaxy population, that becomes dominant (in stellar mass density) at  $z \sim 2$ , while the star-forming population remains almost constant in the redshift

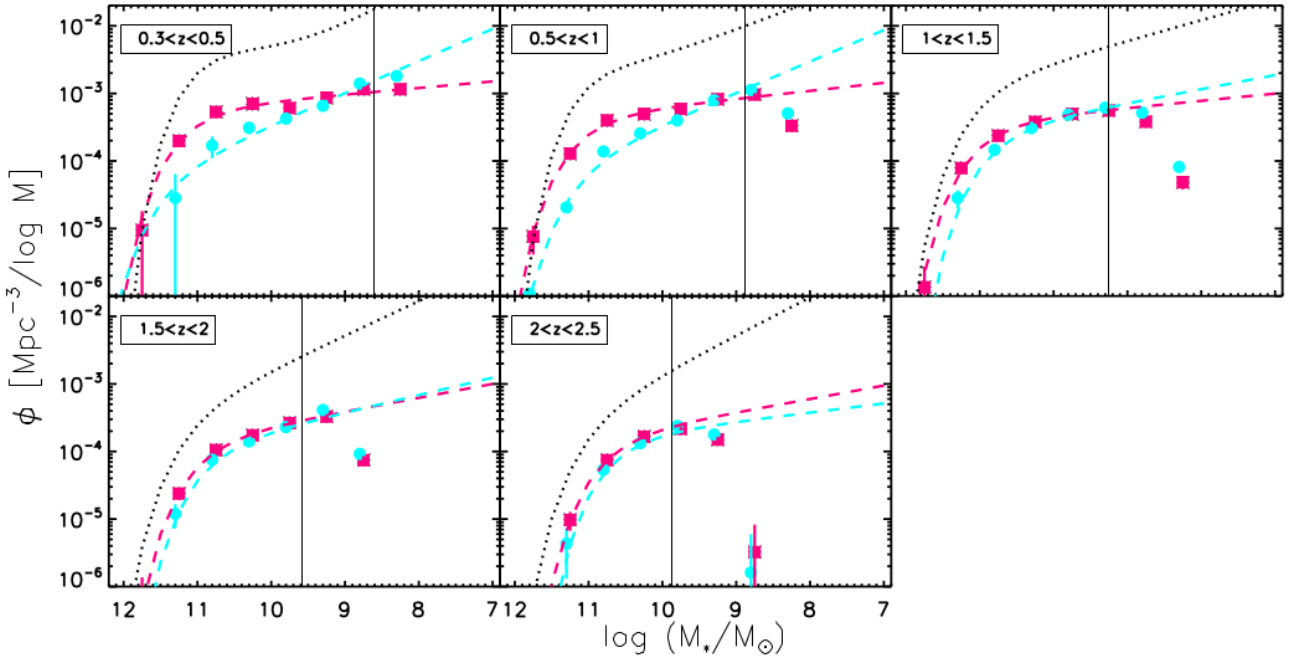


Figure 4.13: Plots from Mortlock et al. (2015): the MF in high (in pink) and low (in blue) densities in the UDS sample. The vertical line is the stellar mass limit of the UDS from Hartley et al. (2013). The dotted black curves are the Schechter fits to the global MF from the relevant redshift bin.

interval studied.

Considering blue/red classification as a proxy for star-forming/quiescent populations, while star-forming galaxies do not show significant evolution in mass and density, also evident in the stellar mass density, quiescent galaxies become more massive with time, in the two extremes of the mass regime. The flattening of the low mass end for red galaxies (increasing the stellar mass density with time), combined with the increasing in  $\phi$  for the higher mass bins shows that there are two separate high-mass and low-mass populations growing in stellar mass, leading to a double Schechter function form in the quenched galaxies MF at low redshift. The massive end formed, built up their stellar mass and quenched earlier, whereas the low mass end slope quick evolution shows the subsequent migration of low-mass galaxies from the blue cloud, especially at  $z < 1.5$  in redshift range studied. They claim that these two quenched populations would be quenched predominantly via different processes. The high-mass end would be mass quenched, while the low-mass end, would undergo environmental quenching.

Figure 4.13 shows the MF for the two environments defined by Mortlock et al. (2015). At higher redshifts ( $z > 1.5$ ) the MFs for different environments are virtually identical, showing that the environment had not a strong impact on galaxies at higher redshifts. This is expected since the densest galaxy clusters have yet to form at that epoch. Only for  $z < 1$  the MFs start to be significantly different. At this epoch, the high mass end starts to be dominated by galaxies living in denser environments, while the low mass galaxies start to be more likely found in lower density regions. These results are in agreement with those found in previous works (e.g., Ilbert et al., 2006b; Bolzonella et al., 2010).

In order to trace the link between quenching and environment, the MF was recalculated, exclusively for the quenched galaxies (red galaxies in the color classification mentioned above), for the two environments considered. The evolution of Schechter parameters is shown in Figure 4.14. The  $\alpha$  evolution (right panel) shows a steeper low-mass slope in high-density environments, compared to low-density environments, for the red galaxies. Despite the large uncertainties, this result corroborates the theory of environment quenching. Low-mass satellite galaxies would exhaust their star formation fuel by environmental processes, as ram pressure stripping or ha-

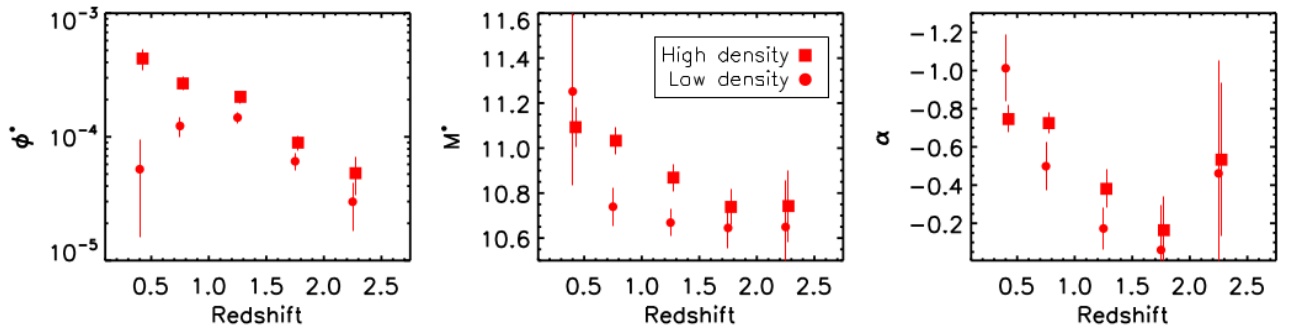


Figure 4.14: Plots from Mortlock et al. (2015): evolution of the Schechter fit parameters for a subsample containing only red galaxies, for high-(squares) and low-(circles) density environments.

rassment. In that sense, it would be reasonable to expect a steeper faint end slope for red galaxies in higher density environments. The higher  $\mathcal{M}^*$  for red galaxies in higher densities, compared to lower densities, indicates that such environments are decisive in the build-up of high-mass red galaxies. The excess of quenched galaxies in high densities links environment to the cessation of star formation.

The last work to be addressed in this timeline is a very recent in a paper published in the beginning of this year (Davidzon et al., 2016). They used more than 50,000 objects with multi-wavelength photometry and spectroscopic redshifts from VIMOS Public Extragalactic Redshift Survey (VIPERS, Guzzo et al., 2014), in the redshift range  $0.5 < z < 0.9$ , over an area of  $\sim 10 \text{ deg}^2$ , to study the effects of the environment in the shape of galaxy stellar MF.

In this work, environments were measured in terms of the 3D density contrast ( $\delta$ ) and two regimes were studied: lowest ( $\delta < 0.7$ ) and highest ( $\delta > 4$ ) densities. Galaxy types were defined as passive, active and intermediate, based on the locus occupied in the color-color diagram ( $r-K$  versus  $NUV-r$ ), as described by Arnouts et al. (2013). Stellar masses was estimated via SED fitting, by using synthetic templates from Bruzual and Charlot (2003). A stellar mass minimum

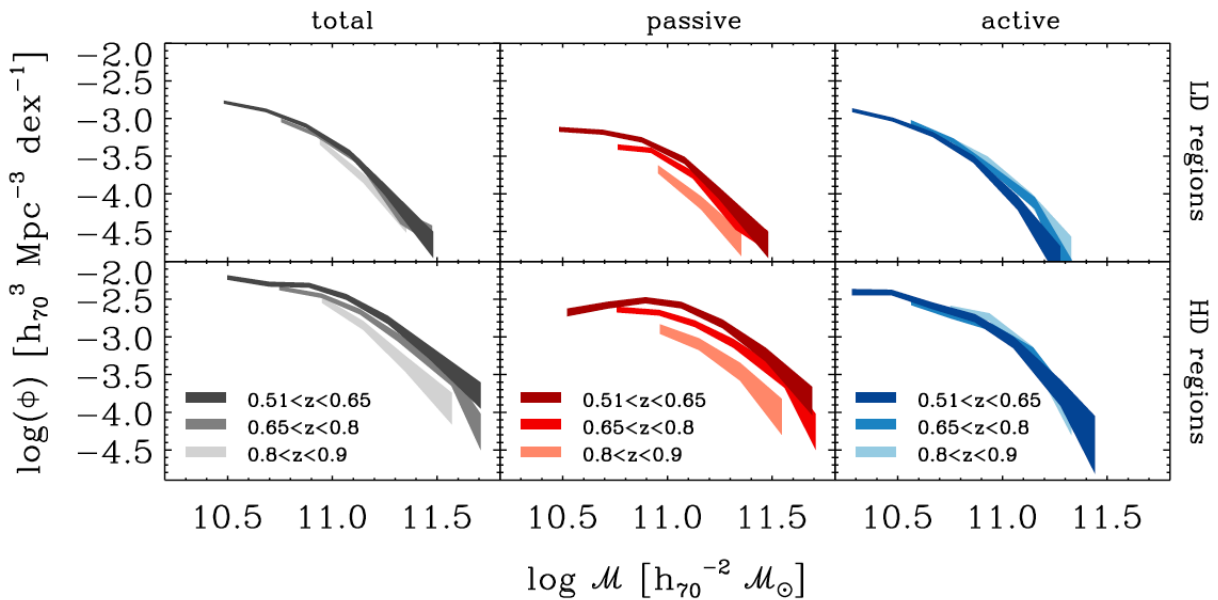


Figure 4.15: Plots from Davidzon et al. (2016): evolution of the MF in the two VIPERS environments, for stellar masses above the completeness limit. Total, passive, and active samples are in black, red, and blue, respectively. Each shaded corresponds to Poissonian uncertainties from the  $1/V_{max}$  method.

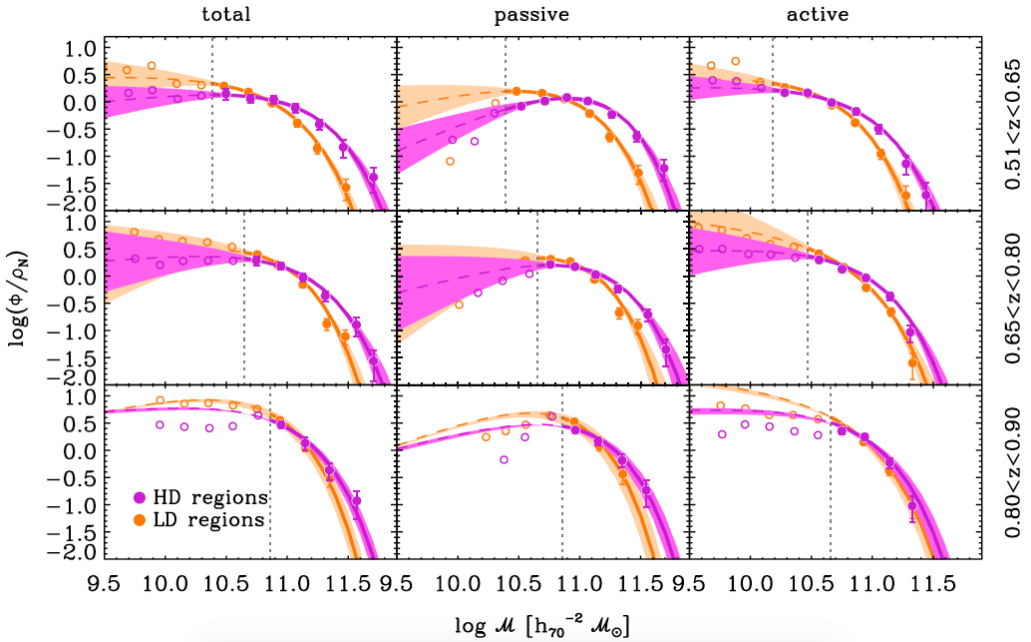


Figure 4.16: Plots from Davidzon et al. (2016): MF of galaxies at low density (orange) and high density (violet) in three different redshift bins. Left, middle and right panels refers to the total sample, only passive and only active (star formation) galaxies, respectively. Vertical dotted lines locate the stellar masses completeness limits in each bin. To compare MF shapes for low and high density environments, the functions were renormalized in such a way that their number density is equal to unity when it is integrated at  $M > M_{lim}$ .

threshold ( $M_{lim}$ ) were adopted, depending on the survey's magnitude limit, redshift, and galaxy type, as described in Pozzetti and Mannucci (2000). The MF was calculated using two different estimators:  $1/V_{max}$  and STY. The results obtained with the two methods are consistent with each other, for  $M > M_{lim}$ , and disagree for  $M < M_{lim}$ , showing that the values for  $M_{lim}$  were fairly estimated. The MF for different environments was normalized to the comoving volume occupied by the corresponding environment. This correction solves the issue raised by Zucca et al. (2009), allowing direct comparison between the values of  $\phi^*$  from different environments.

MF evolution is strong in high densities between  $0.5 \lesssim z \lesssim 0.9$ , while in low-density it is nearly constant for the same redshift range, as shown in Figure 4.15. MFs in high and low-density environments have different shapes. Figure 4.16 brings the same results of Figure 4.15, but reorganized to facilitate the comparison between the MF for different environments. The most massive galaxies are preferably found in denser environments since the high-density MF dominates the high-mass end after  $z \sim 0.7$ . Before that, in the highest redshift bin, the MF is very similar for both environments, above the completeness limit. There is a hint that the MF low-mass end is flatter in the high-density regions with a pronounced decreasing for passive galaxies, but this result must be looked carefully, due to the large uncertainties in this mass regime.

Since the interpretation of the results are limited by the uncertainties in the observed data, that are considerably larger for galaxies with masses below the stellar mass completeness limit of the survey, Davidzon et al. (2016) also investigated these environmental trends by using mock catalogs derived from the Millennium simulation, keeping the same definitions of galaxy environments as done in the real survey.

The same trend noticed in the low-mass end slope for real galaxies is also observed in the mock MF. It can be related to a larger number of mergers in higher density environments. Analyzing the high-mass end of the mock MF, the higher number of massive galaxies in dense regions is linked to a large number of massive halos ( $M_{halo} > 10^{13} M_\odot$ ). Such massive halos are not present in the lower-density sample. In summary, the environmental classification based on the galaxy

density contrast is, in some way, a classification that also separates distinct halo properties. This emphasizes the ambiguity of the “mass vs. environment” dichotomy.

As it was concluded in several previous works, the differences between lower and higher density environment weaken with increasing redshift. This trend is expected to continue at higher redshifts, where the massive systems that correspond to the densest environments observed in the local Universe have not collapsed yet.

## Chapter 5

# Summary and Conclusions

Galaxies are not homogeneously distributed in the Universe (on the scale of hundreds or thousands of megaparsecs). Instead, some of them live clustered in overdense regions and the rest is found spread in the field. In the local Universe, we observe remarkable differences between the galaxy populations that live in these two environments. However, in the far past, these differences were not so significant, or even nonexistent. Hence, we can conclude that the history was not the same in the different environments. Galaxy evolution ran different paths in clusters and in the field, which culminates in the observed dichotomy between galaxy properties in these two extremes.

In the field, galaxies are far from their neighbors, so the evolution occurs mainly driven by internal secular processes. Mergers can happen, but they become progressively unlike as the Universe expands. Field galaxies are not closed systems since they exchange energy and matter with the IGM via inflows and outflows, but the interaction between galaxies is not relevant to understand their evolution. For these objects, *Nature* speaks louder than *Nurture*. Alternatively, mergers were very common in the early Universe in overdense regions, during the formation of the progenitor systems that would become the galaxy clusters as we know in the present day. The immediate consequence of this fact is the well-known morphology-density relation. Clusters are filled with red, quiescent, early-type galaxies, while the field is dominated by blue, star-forming, late-type galaxies.

In clusters, the proximity of galaxies allows to several kinds of interactions that strongly affect the galaxy evolution e.g., ram-pressure stripping, harassment, tidal effects, strangulation and galactic cannibalism. Therefore, clusters have developed peculiarities, that are not observed in the field, like giant galaxies with extended envelopes and the intraccluster light.

In order to understand the dependence of galaxy evolution on the environment, extragalactic surveys have observed and measured galaxy properties in different epochs (given by the redshift) and in regions with different number densities. Due to the current observational limitations, most of them did not have high redshift samples with powerful statistics, so they have limited their analysis up to  $z \sim 1$ , or a little bit far. Some of their findings are commented below.

Galaxies have been, in general, dimming since  $z \sim 1$ . The characteristic magnitude  $M^*$  is fading over time, for both early/late-type populations (e.g., Ilbert et al., 2006b; Faber et al., 2007; Zucca et al., 2009). This is a consequence of the decreasing in the average SFR during in the correspondent epoch (Madau et al., 1998).

About the number of objects with magnitude around  $M^*$  or masses around  $\mathcal{M}^*$ , reflected in the number density  $\phi^*$ , there is some disagreement in the results found in the literature. In some

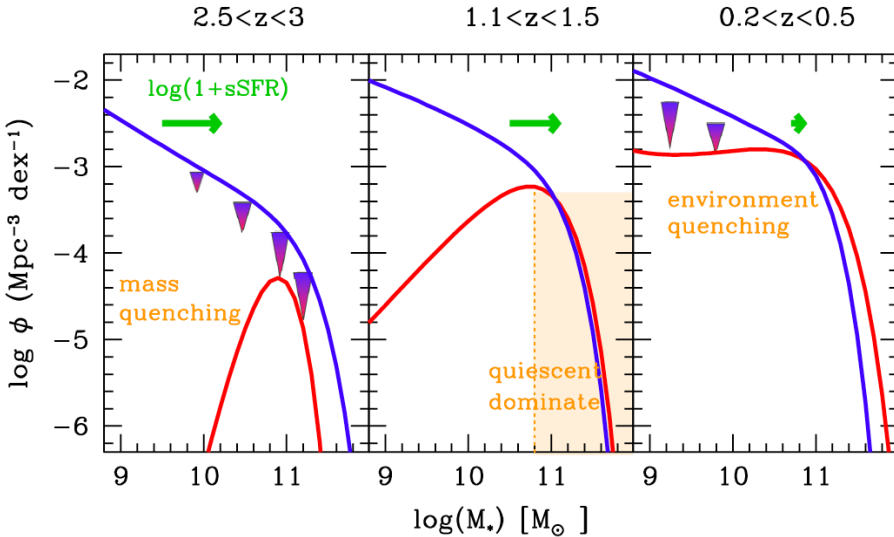


Figure 5.1: Figure from Ilbert et al. (2013) how specific SFR and quenching impact the MF for star-forming(blue) and quiescent (red). The large arrows represent quenching. The green arrows correspond to the mass increase expected in 2 Gyr by the model considered in the paper.

works it has been virtually constant over time since  $z \sim 1$  (e.g., Ilbert et al., 2006b; Mortlock et al., 2015; Davidzon et al., 2016) or slightly decreasing (e.g., Zucca et al., 2009) for the blue galaxies. For red galaxies, Zucca et al. (2009); Mortlock et al. (2015); Davidzon et al. (2016) found an increase over time, while Ilbert et al. (2006b) found it also constant. Mortlock et al. (2015) argue that  $\phi^*$  must always increase with time because galaxies have been always building up mass, by mergers or gas accretion. In all works addressed, the authors consider that a fraction of late-type galaxies are transformed into early-type galaxies over time and this transformation is more efficient in overdense regions.

The luminosity density has decreased since  $z \sim 1.5$  for blue galaxies, but increased in the past for red galaxies, reaching a peak around  $z \sim 0.9$ . This is due to an interplay between the grow in number (blue galaxies merging and transforming into red galaxies) and the progressive loss in luminosity (decreasing the star-formation activity) Ilbert et al. (2006b).

The morphology-density (or color-density) relation has been confirmed recently by several authors. The field is dominated by faint blue objects, while the brightest red galaxies are more likely to be found in overdense regions (Balogh et al., 2001; Ilbert et al., 2006a; Zucca et al., 2009; Bolzonella et al., 2010; Mortlock et al., 2015; Davidzon et al., 2016).

Some authors found that the important changes in some observables happened before  $z \sim 1$ , as the LF shape in clusters (Kodama and Bower, 2003), the color-density relation (Cucciati et al., 2006), the SFR (Cucciati et al., 2006), the fraction of blue/red galaxies in different environments (Gerke et al., 2007; Bolzonella et al., 2010). At lower ranges of redshift, these properties are relatively stable. Evolutionary processes like the morphological transformation of disks into ellipticals and the migration from the blue cloud to the red sequence in the CMD started before and happen quicker in clusters than in the field (even more quickly for the most massive galaxies in cluster cores). The field's history has a delay of  $\sim 2$  Gyr compared to clusters' (Bolzonella et al., 2010). In the field, changes happen slowly and still significant in the present day (Zucca et al., 2009).

Other works showed properties that were common for under and overdense regions at  $z \lesssim 1$  but have differentiated since then, as the LF shapes (Ilbert et al., 2006b), the MF shape (Bolzonella et al., 2010; Davidzon et al., 2016), and the MF high-mass end dominant type (Mortlock et al., 2015). The authors claim that this progressive differentiation between environments is a consequence of previous processes, that begun at higher redshifts. For instance, Gerke et al. (2007) argue that galaxy groups became suitable for quenching at  $z \sim 2$ , but the subsequent change in the fraction of blue galaxies become significant later, in  $z \sim 1$ .

The processes that cause the quenching of the star-formation activity are different in nature, so they can be divided into two categories: “mass quenching” and “environmental quenching”. In

the first case, very massive galaxies tend to evolve rapidly, simply due to gravity. The more initial mass, the faster the collapse and gas consuming. This “mass quenching” affects substantially the high-mass end of the MF, that shows significant evolution as higher redshifts. At later times, the environmental processes become more efficient in suppressing the star formation and it affects more the low-mass galaxies, reflecting in a significant evolution of the low-mass end slope (as represented in the sketch in Figure 5.1). Although these two phenomena are more efficient in different epochs, they are not separable. The ambiguity between mass and environment is “unresolvable” because the probability for a galaxy to have a given mass is totally linked to the probability to be found in a given density environment.

# Bibliography

- G. O. Abell. The Distribution of Rich Clusters of Galaxies. *ApJS*, 3:211, May 1958. doi: 10.1086/190036.
- J. Annis, S. Bridle, F. J. Castander, et al. Constraining Dark Energy with the Dark Energy Survey: Theoretical Challenges. *ArXiv Astrophysics e-prints*, October 2005.
- S. Arnouts, E. Le Floc'h, J. Chevallard, et al. Encoding of the infrared excess in the NUVrK color diagram for star-forming galaxies. *AAp*, 558:A67, October 2013. doi: 10.1051/0004-6361/201321768.
- M. L. Balogh, D. Christlein, A. I. Zabludoff, et al. The Environmental Dependence of the Infrared Luminosity and Stellar Mass Functions. *ApJ*, 557:117–125, August 2001. doi: 10.1086/321670.
- S. V. W. Beckwith, M. Stiavelli, A. M. Koekemoer, et al. The Hubble Ultra Deep Field. *AJ*, 132:1729–1755, November 2006. doi: 10.1086/507302.
- N. Benitez, R. Dupke, M. Moles, et al. J-PAS: The Javalambre-Physics of the Accelerated Universe Astrophysical Survey. *ArXiv e-prints*, March 2014.
- L. Bianchi et al. The Galaxy Evolution Explorer (GALEX): an All Sky Ultraviolet Survey. *MEMSAI*, 70, 1999.
- B. Binggeli, A. Sandage, and G. A. Tammann. The luminosity function of galaxies. *ARAA*, 26:509–560, 1988. doi: 10.1146/annurev.aa.26.090188.002453.
- J. Binney and S. Tremaine. *Galactic dynamics*. 1987.
- M. Bolzonella, K. Kovač, L. Pozzetti, et al. Tracking the impact of environment on the galaxy stellar mass function up to  $z \sim 1$  in the 10 k zCOSMOS sample. *AAp*, 524:A76, December 2010. doi: 10.1051/0004-6361/200912801.
- H. Bravo-Alfaro, V. Cayatte, J. H. van Gorkom, et al. VLA H I Imaging of the Brightest Spiral Galaxies in Coma. *AJ*, 119: 580–592, February 2000. doi: 10.1086/301194.
- G. Bruzual and S. Charlot. Stellar population synthesis at the resolution of 2003. *MNRAS*, 344:1000–1028, October 2003. doi: 10.1046/j.1365-8711.2003.06897.x.
- H. Butcher and A. Oemler, Jr. The evolution of galaxies in clusters. V - A study of populations since Z approximately equal to 0.5. *ApJ*, 285:426–438, October 1984. doi: 10.1086/162519.
- C. A. Collins, J. P. Stott, M. Hilton, S. T. Kay, S. A. Stanford, M. Davidson, M. Hosmer, B. Hoyle, A. Liddle, E. Lloyd-Davies, R. G. Mann, N. Mehrtens, C. J. Miller, R. C. Nichol, A. K. Romer, M. Sahlén, P. T. P. Viana, and M. J. West. Early assembly of the most massive galaxies. *Nature*, 458:603–606, April 2009. doi: 10.1038/nature07865.
- C. J. Conselice, A. Wilkinson, K. Duncan, et al. The Evolution of Galaxy Number Density at  $z < 8$  and Its Implications. *ApJ*, 830:83, October 2016. doi: 10.3847/0004-637X/830/2/83.
- R. Content, A. Cimatti, M. Robberto, et al. Offspring of SPACE: the spectrograph channel of the ESA Dark Energy Mission EUCLID. In *Space Telescopes and Instrumentation 2008: Optical, Infrared, and Millimeter*, volume 7010 of *procspie*, page 70104S, July 2008. doi: 10.1117/12.805409.
- L. L. Cowie, A. Songaila, E. M. Hu, et al. New Insight on Galaxy Formation and Evolution From Keck Spectroscopy of the Hawaii Deep Fields. *AJ*, 112:839, September 1996. doi: 10.1086/118058.
- O. Cucciati, A. Iovino, C. Marinoni, et al. The VIMOS VLT Deep Survey: the build-up of the colour-density relation. *AAp*, 458: 39–52, October 2006. doi: 10.1051/0004-6361:20065161.
- I. Davidzon, O. Cucciati, M. Bolzonella, et al. The VIMOS Public Extragalactic Redshift Survey (VIPERS). Environmental effects shaping the galaxy stellar mass function. *AAp*, 586: A23, February 2016. doi: 10.1051/0004-6361/201527129.
- G. De Lucia and J. Blaizot. The hierarchical formation of the brightest cluster galaxies. *MNRAS*, 375:2–14, February 2007. doi: 10.1111/j.1365-2966.2006.11287.x.
- A. Dressler. Galaxy morphology in rich clusters - Implications for the formation and evolution of galaxies. *ApJ*, 236:351–365, March 1980. doi: 10.1086/157753.
- O. J. Eggen, D. Lynden-Bell, and A. R. Sandage. Evidence from the motions of old stars that the Galaxy collapsed. *ApJ*, 136: 748, November 1962. doi: 10.1086/147433.
- D. J. Eisenstein, D. H. Weinberg, E. Agol, et al. SDSS-III: Massive Spectroscopic Surveys of the Distant Universe, the Milky Way, and Extra-Solar Planetary Systems. *AJ*, 142:72, September 2011. doi: 10.1088/0004-6256/142/3/72.
- P. B. Eskridge, J. A. Frogel, R. W. Pogge, et al. The Frequency of Barred Spiral Galaxies in the Near-Infrared. *AJ*, 119:536–544, February 2000. doi: 10.1086/301203.
- S. M. Faber, C. N. A. Willmer, C. Wolf, et al. Galaxy Luminosity Functions to  $z \sim 1$  from DEEP2 and COMBO-17: Implications for Red Galaxy Formation. *ApJ*, 665:265–294, August 2007. doi: 10.1086/519294.
- R. Farouki and S. L. Shapiro. Computer simulations of environmental influences on galaxy evolution in dense clusters. II - Rapid tidal encounters. *ApJ*, 243:32–41, January 1981. doi: 10.1086/158563.
- B. Flaugher et al. The Dark Energy Survey. *International Journal of Modern Physics A*, 20:3121–3123, 2005. doi: 10.1142/S0217751X05025917.
- J. S. Gallagher, III and J. P. Ostriker. A Note on Mass Loss during Collisions between Galaxies and the Formation of Giant Systems. *AJ*, 77:288, May 1972. doi: 10.1086/111280.
- B. F. Gerke, J. A. Newman, S. M. Faber, et al. The DEEP2 galaxy redshift survey: the evolution of the blue fraction in groups and the field. *MNRAS*, 376:1425–1444, April 2007. doi: 10.1111/j.1365-2966.2007.11374.x.

- M. D. Gladders and H. K. C. Yee. A New Method For Galaxy Cluster Detection. I. The Algorithm. *AJ*, 120:2148–2162, October 2000. doi: 10.1086/301557.
- T. S. Gonçalves, D. C. Martin, K. Menéndez-Delmestre, et al. Quenching Star Formation at Intermediate Redshifts: Down-sizing of the Mass Flux Density in the Green Valley. *ApJ*, 759:67, November 2012. doi: 10.1088/0004-637X/759/1/67.
- J. E. Gunn and J. R. Gott, III. On the Infall of Matter Into Clusters of Galaxies and Some Effects on Their Evolution. *ApJ*, 176:1, August 1972. doi: 10.1086/151605.
- L. Guzzo, M. Scoville, B. Garilli, et al. The VIMOS Public Extragalactic Redshift Survey (VIPERS). An unprecedented view of galaxies and large-scale structure at  $0.5 < z < 1.2$ . *AAp*, 566:A108, June 2014. doi: 10.1051/0004-6361/201321489.
- W. G. Hartley, O. Almaini, A. Mortlock, et al. Studying the emergence of the red sequence through galaxy clustering: host halo masses at  $z > 2$ . *MNRAS*, 431:3045–3059, June 2013. doi: 10.1093/mnras/stt383.
- Y. Hashimoto, A. Oemler, Jr., H. Lin, and OTHERS. The Influence of Environment on the Star Formation Rates of Galaxies. *ApJ*, 499:589–599, May 1998.
- E. Hubble and M. L. Humason. The Velocity-Distance Relation among Extra-Galactic Nebulae. *ApJ*, 74:43, July 1931. doi: 10.1086/143323.
- O. Ilbert, S. Arnouts, H. J. McCracken, et al. Accurate photometric redshifts for the CFHT legacy survey calibrated using the VIMOS VLT deep survey. *AAp*, 457:841–856, October 2006a. doi: 10.1051/0004-6361:20065138.
- O. Ilbert, O. Cucciati, C. Marinoni, et al. Evidence for environment-dependent galaxy Luminosity Function up to  $z=1.5$  in the VIMOS-VLT Deep Survey. *ArXiv Astrophysics e-prints*, February 2006b.
- O. Ilbert, H. J. McCracken, O. Le Fèvre, et al. Mass assembly in quiescent and star-forming galaxies since  $z \sim 4$  from UltraVISTA. *AAp*, 556:A55, August 2013. doi: 10.1051/0004-6361/201321100.
- Z. Ivezić, J. A. Tyson, T. Axelrod, et al. LSST: From Science Drivers To Reference Design And Anticipated Data Products. In *American Astronomical Society Meeting Abstracts #213*, volume 41 of *Bulletin of the American Astronomical Society*, page 366, January 2009.
- F. Jiang and F. C. van den Bosch. Generating merger trees for dark matter haloes: a comparison of methods. *MNRAS*, 440:193–207, May 2014. doi: 10.1093/mnras/stu280.
- T. Kodama and R. Bower. The  $K_s$ -band luminosity and stellar mass functions of galaxies in  $z \sim 1$  clusters. *MNRAS*, 346:1–12, November 2003. doi: 10.1046/j.1365-2966.2003.07093.x.
- J. Kormendy. *Secular Evolution in Disk Galaxies*, page 1. October 2013.
- J. Kormendy and R. Bender. A Proposed Revision of the Hubble Sequence for Elliptical Galaxies. *ApJL*, 464:L119, June 1996. doi: 10.1086/310095.
- J. Kormendy and R. Bender. A Revised Parallel-sequence Morphological Classification of Galaxies: Structure and Formation of S0 and Spheroidal Galaxies. *ApJS*, 198:2, January 2012. doi: 10.1088/0067-0049/198/1/2.
- J. Kormendy and R. C. Kennicutt, Jr. Secular Evolution and the Formation of Pseudobulges in Disk Galaxies. *ARAA*, 42:603–683, September 2004. doi: 10.1146/annrev.astro.42.053102.134024.
- J. D. Kurk, H. J. A. Röttgering, L. Pentericci, et al. A Search for clusters at high redshift. I. Candidate Lyalpha emitters near 1138–262 at  $z=2.2$ . *AAp*, 358:L1–L4, June 2000.
- R. B. Larson, B. M. Tinsley, and C. N. Caldwell. The evolution of disk galaxies and the origin of S0 galaxies. *ApJ*, 237:692–707, May 1980. doi: 10.1086/157917.
- O. Le Fèvre, G. Vettolani, B. Garilli, et al. The VIMOS VLT deep survey. First epoch VVDS-deep survey: 11 564 spectra with  $17.5 \leq \text{IAB} \leq 24$ , and the redshift distribution over  $0 \leq z \leq 5$ . *A&A*, 439:845–862, September 2005. doi: 10.1051/0004-6361:20041960.
- G. Lemson and t. Virgo Consortium. Halo and Galaxy Formation Histories from the Millennium Simulation: Public release of a VO-oriented and SQL-queryable database for studying the evolution of galaxies in the LambdaCDM cosmogony. *ArXiv Astrophysics e-prints*, August 2006.
- S. J. Lilly, O. Le Fèvre, A. Renzini, et al. zCOSMOS: A Large VLT/VIMOS Redshift Survey Covering  $0 \leq z \leq 3$  in the COSMOS Field. *ApJS*, 172:70–85, September 2007. doi: 10.1086/516589.
- G. B. Lima Neto. *Astronomia Extragalactica*. 2016.
- C. C. Lin and F. H. Shu. On the Spiral Structure of Disk Galaxies, II. Outline of a Theory of Density Waves. *Proceedings of the National Academy of Science*, 55:229–234, February 1966.
- J. Loveday, P. Norberg, I. K. Baldry, et al. Galaxy and Mass Assembly (GAMA): ugriz galaxy luminosity functions. *MNRAS*, 420:1239–1262, February 2012. doi: 10.1111/j.1365-2966.2011.20111.x.
- P. Madau and M. Dickinson. Cosmic Star-Formation History. *ARAA*, 52:415–486, August 2014. doi: 10.1146/annrev-astro-081811-125615.
- P. Madau, L. Pozzetti, and M. Dickinson. The Star Formation History of Field Galaxies. *ApJ*, 498:106–116, May 1998. doi: 10.1086/305523.
- T. McNaught-Roberts, P. Norberg, C. Baugh, et al. Galaxy And Mass Assembly (GAMA): the dependence of the galaxy luminosity function on environment, redshift and colour. *MNRAS*, 445:2125–2145, December 2014. doi: 10.1093/mnras/stu1886.
- S. Mei, B. P. Holden, J. P. Blakeslee, et al. Evolution of the Color-Magnitude Relation in Galaxy Clusters at  $z \sim 1$  from the ACS Intermediate Redshift Cluster Survey. *ApJ*, 690:42–68, January 2009. doi: 10.1088/0004-637X/690/1/42.
- A. J. Mendez, A. L. Coil, J. Lotz, et al. AEGIS: The Morphologies of Green Galaxies at  $0.4 < z < 1.2$ . *ApJ*, 736:110, August 2011. doi: 10.1088/0004-637X/736/2/110.
- C. J. Miller, R. C. Nichol, D. Reichart, et al. The C4 Clustering Algorithm: Clusters of Galaxies in the Sloan Digital Sky Survey. *AJ*, 130:968–1001, September 2005. doi: 10.1086/431357.
- H. Mo, F. C. van den Bosch, and S. White. *Galaxy Formation and Evolution*. May 2010.
- A. Mortlock, C. J. Conselice, W. G. Hartley, et al. Deconstructing the galaxy stellar mass function with UKIDSS and CANDELS: the impact of colour, structure and environment. *MNRAS*, 447:2–24, February 2015. doi: 10.1093/mnras/stu2403.
- J. A. Newman, M. C. Cooper, M. Davis, et al. The DEEP2 Galaxy Redshift Survey: Design, Observations, Data Reduction, and Redshifts. *ApJs*, 208:5, September 2013. doi: 10.1088/0067-0049/208/1/5.